



HAL
open science

Dynamic rate and channel use allocation for cooperative wireless networks

Ali Al Khansa, Stefan Cerovic, Raphael Visoz, Yezekael Hayel, Samson Lasaulce

► **To cite this version:**

Ali Al Khansa, Stefan Cerovic, Raphael Visoz, Yezekael Hayel, Samson Lasaulce. Dynamic rate and channel use allocation for cooperative wireless networks. EURASIP Journal on Wireless Communications and Networking, 2023, 2023 (1), pp.51. 10.1186/s13638-023-02243-6 . hal-04131857

HAL Id: hal-04131857

<https://hal.science/hal-04131857v1>

Submitted on 17 Jun 2023

HAL is a multi-disciplinary open access archive for the deposit and dissemination of scientific research documents, whether they are published or not. The documents may come from teaching and research institutions in France or abroad, or from public or private research centers.

L'archive ouverte pluridisciplinaire **HAL**, est destinée au dépôt et à la diffusion de documents scientifiques de niveau recherche, publiés ou non, émanant des établissements d'enseignement et de recherche français ou étrangers, des laboratoires publics ou privés.



Distributed under a Creative Commons Attribution 4.0 International License

RESEARCH

Open Access



Dynamic rate and channel use allocation for cooperative wireless networks

Ali Al Khansa^{1,2*} , Stefan Cerovic³, Raphael Visoz^{1*}, Yezekael Hayel² and Samson Lasaulce⁴

*Correspondence:
akhansa17@gmail.com; raphael.
visoz@orange.com

¹ Orange Innovation, Chatillon,
France

² LIA, Avignon University,
Avignon, France

³ Ericsson, Massy, France

⁴ CRAN, CNRS,
Vandoeuvre-les-Nancy, France

Abstract

In this paper, we investigate the performance of link adaptation (LA) algorithms for cooperative multiple access multiple relay networks. In the first transmission phase, the sources transmit in turn in consecutive time slots. In the second cooperative retransmission phase, the destination schedules one relaying node to send redundancies. LA is a fundamental mechanism allowing the source nodes to adapt to the radio channel conditions. In this paper, we investigate the problem of rate allocation using a centralized method, where the destination is the central node that determines the source rates. Furthermore, and in sharp contrast with existing cooperative transmission schemes, we consider the packet size to be time-varying. In other words, we propose adapting the slot duration of each of the sources during the transmission phase as a new degree of freedom. Accordingly, the LA process determines the rate and the time slot duration of each source. We consider a practical performance metric namely, the network spectral efficiency. This metric being difficult to be optimized (given the complex multi-variable optimization problem), we propose best-response dynamic (BRD) algorithms to solve the rate and time duration allocation. Then, we conduct a thorough performance analysis using Monte-Carlo simulations. Our numerical results validate the effectiveness of the proposed BRD algorithms as they yield performance close to the corresponding exhaustive search approach. Furthermore, the results ensure the gain of exploiting the new degree of freedom of the variable slot duration.

Keywords: Slow-link adaptation, Fast-link adaptation, Best-response dynamics, Multi-source multi-relay wireless network, QoS target, Spectral efficiency

1 Introduction

Cooperative communications [1] represent one of the key physical layer technologies that are being investigated, and this is due to their significant impact on the spectral efficiency of wireless channels. The concept behind cooperative communications is to let sources share their resources with the aim of improving the transmission and reception processes. This kind of communication network is seen in different nowadays scenarios as for example in some unmanned aerial vehicle (UAV) systems [2, 3].

In this paper, we aim to study the rate and the channel use allocation for cooperative networks. We present practical algorithms that perform resource allocation strategies applicable in different scenarios and different radio conditions. There are different

factors that affect the resource allocation for cooperative networks, such as the network nature, the relaying protocol used, and the methods used in allocation. In this introduction Section, we first present the state of the art of the different cooperative networks, followed by the prior art of relaying protocols. Then, we shed the light on different resource allocation problems in cooperative and non-cooperative networks, where different methods are used. Finally, in the last subsection of the introduction, we present in details the scope of this paper.

1.1 Motivations and different cooperative networks

From a historical point of view, cooperative communications go back to the year 1970, where van der Meulen derived the upper and lower bounds of the channel capacity of a TRN [4]. In this reference, we see some fundamental principles related to cooperative communication. Then, other relay channels and further cooperative networks were investigated as in [5]. Remarkable work on relaying was done by Cover and El Gammal in several publications as in [5–7]. Using the min-cut max-flow capacity upper bound, the capacity is established for degraded and reversely degraded feedback relay channels. So far, the main results of these works have not been surpassed.

Basically, the system model of cooperative communication channels is composed of three main components: source, relay, and destination nodes. According to the number of each of these elements, the nature of the cooperative channel is determined. For a multiple number of relays, the TRN can be extended to MRN consisting of a single source, a single destination, and multiple relay nodes. Such kind of channels is investigated in [7–9]. A RBN is composed of a single source, a single relay, and multiple destination nodes [10]. As a natural counterpart of the RBN, the MARN is composed of multiple source nodes, with a single relay, and a single destination [11–13]. In the mentioned networks, several problems are investigated in the prior art.

In this paper, we consider the MAMRN composed of multiple source nodes, multiple relay nodes and a single destination. This system can be seen as a generalization of the previously mentioned systems, except for the RBC which includes multiple destination nodes. The considered system is seen in nowadays applications. In [2] for example, it is stated that the considered structure (i.e., the MAMRN) is the main topology structure for UAV cooperative surveillance networks. However, it is seen in [10] that the capacity region of the general MAMRN is still unknown. In MAMRN, the multiple access can be either orthogonal (as considered in this paper and in other works: [16]) or non-orthogonal (as in [15]), where orthogonality may be achieved through time, frequency, or code division multiplexing.

Throughout the different prior arts that targeted the MAMRN, two major (recent) works are the ones done in the theses [14] and [15]. In [15], the outage analysis of different examples of MAMRN is presented (check [17–19]). The analysis covers different coding and decoding schemes as well as different transmission scenarios (orthogonal and non-orthogonal). Also in [15], several selection strategies are proposed for the MAMRN (check [20]). In [14], further contributions are presented related to the MAMRN while focusing on orthogonal MAMRN. Three main problems are investigated: resource

allocation problems, relaying nodes selection strategies (check [21]), and control exchange process problems (check [22]).

In this paper, user cooperation is considered, where a user that does not have a message to send, acts as a relay node in order to improve the performance [22]. The relaying nodes (i.e., the sources and the relays) are assumed half-duplex; they can listen to each other while not transmitting. The concept of user cooperation was introduced in the work of Sendonaris et al. [23, 24] where it is sometimes referred to by “cooperative diversity” [25]. In these works, user cooperation is seen as a promising method that has significant gains in various performance metrics (i.e., outage probability, diversity gain, multiplexing gain, diversity-multiplexing trade-off, etc.). We summarize the mentioned cooperative networks in Table 1.

1.2 Different relaying protocols

In our work, relaying nodes apply the selective decode-and-forward (SDF) relaying protocol (RP), which means that they can forward only a signal representative of successfully decoded source messages. The error detection is based on cyclic redundancy check (CRC) bits that are appended to each source message. The SDF relaying protocol is an advanced version of the Decode-and-forward (DF) RP. The principle of DF protocol is introduced in [5], where unlike SDF, cooperative nodes are obliged to wait to successfully decode all the source messages before starting to cooperate. In [9], an orthogonal multiple DF relaying network was presented, in which a diversity analysis and error probability derivation was carried out. In [26], the problem of resource allocation in DF cooperative communication networks was investigated, considering a limited rate feedback channel. SDF belongs to the category of non-linear (regenerative) relaying protocols.

Other commonly used protocols in the literature that belong to the same category are compress-and-forward (CF) [28, 29], compute-and-forward (CoF) [30, 31], and quantize-map-and-forward (QMF) [32]. In the CF RP, the relay transmits an estimated version of its observation of the received signal. The relay node uses source coding to exploit the side information available at the destination. In the CoF RP, the relay decodes linear equations of the transmitted messages using the noisy linear combinations provided by the channel. Such a protocol is suitable in multi-source networks where more than one source is included. The QMF RP is another generalization of CF RP, where the estimated version of the signal is based on quantizing the received signal at the noise

Table 1 Different cooperative networks

Cooperative network	References
Three-terminal relay network (TRN)	[4–7]
Multiple relay network (MRN)	[7–10]
Relay broadcast network (RBN)	[10]
Multiple access relay network (MARN)	[11–13]
Multiple access multiple relay network (MAMRN)	[10, 14, 15], This work

level and mapping it to a random Gaussian codeword for forwarding. The final destination decodes the source’s message based on the received signal.

The most famous example of the category of linear relaying protocols is certainly amplify-and-forward (AF) [33, 34], while there exist many other interesting relaying protocols, such as coded cooperation (CC) [35]. In the AF RP, the relay transmits an amplified version of its received message. It can be seen as a repetition code, where a relay is simply forwarding a scaled version of its received signal. For CC, the principle is to partition the codewords of each transmitting node and transmit each part through an independent channel. Other types of relaying protocols are non-orthogonal amplify-and-forward (NOAF) [36] and dynamic decode-and-forward (DDF). These protocols are evaluated in terms of diversity-multiplexing trade-off (DMT) [27]. In DDF, a certain approach is needed to choose the point where the relay switches from listening to transmitting. As this point is not fixed, fountain codes [37] are considered as they do not have a predetermined rate at the transmitter.

Performance evaluation and comparison of the mentioned protocols is done in the literature (e.g., in [38–40]), where we can see that there exist some scenarios where the SDF RP is outperformed by some other protocols. Nevertheless, there is no decisive conclusion in this research area, and rigorous fair comparisons still have to be done for the slow fading half-duplex MAMRN. We summarize the mentioned relaying protocols in Table 2.

Additionally, we assume that joint encoding (network coding) is performed on successfully decoded messages at the relaying nodes. Introduced in [41] for graphical networks, that concept implies that the relaying nodes not only can route or replicate the information received on input links to output links, but they can also encode that information before performing the transmission. The application of network coding to the physical layer of wireless networks is studied in various contributions, with particular attention to the combination of network and channel coding. Example applications in

Table 2 Relaying protocols (RP) summary. The second column *T* represents the *Type*, where *R* and *L* represents *Regenerative* and *Linear* relaying protocols types

Relaying protocol	Type	Method	References
Decode-and-forward (DF)	R	Obligated to wait to decode all sources before starting relaying	[5, 9, 26]
Selective decode-and-forward (SDF)	R	Can switch to relaying before decoding all sources	[22], This Work
Dynamic decode-and-forward (DDF)	R	Switching point between listening and relaying is not fixed	[27]
Compress-and-forward (CF)	R	An estimated version of the received signal is transmitted	[28, 29]
Compute-and-forward (CoF)	R	Uses noisy linear combination to decode transmitted messages	[30, 31]
Quantize-map-and-forward (QMF)	R	A quantized version of the signal is transmitted	[32]
Amplify-and-forward (AF)	L	Repetition code, transmitting amplified version of the signal	[33, 34]
Coded cooperation (CC)	L	Uses partition of the codewords of each transmitting node	[35]
Non-orthogonal AF (NOAF)	L	Uses AF for NOMA to serve primary and secondary users	[36]

MARC, two-way relay channel (TWRC) and user cooperation are given in [42, 43] and [44], respectively. Note that simpler encoding strategies based on existing incremental redundancy channel coding schemes, as described in [22], can be easily taken into account in our general framework.

1.3 Different link adaptation problems

In the prior art, several works tackled the problem of resource allocation [45], such as power allocation problem in cooperative networks [46]. In reference [46] for example, the authors target the power allocation problem from the energy-saving perspective. Another problem is the sub-carrier allocation, where several papers investigated non-cooperative networks [47, 48] and other papers investigated cooperative networks [49]. A survey is presented in [47], where the aim of the channel allocation techniques presented was to reduce contention with energy requirements. In a recent publication [48], the authors propose a novel channel allocation technique that uses artificial intelligence and specifically genetic algorithm. It was found that the optimized result with the help of genetic algorithm was better than the results without using genetic algorithm.

On the other hand, a lot of research interest is seen in the rate allocation problem. In [50], the authors present the capacity region of different networks. The capacity region represents the set of source rates of a network that can possibly be decoded by the destination. Following this definition, we see the link between rate allocation and capacity region analysis. On the other hand, and for the networks where the capacity region is not well-known, the rate allocation problem answers the question of what rate each source should use to improve the transmission and reception. In [51], the rate allocation problem from the perspective of energy efficiency is presented for non-orthogonal multiple access (NOMA) networks. In [52], on the other hand, a dynamic sensor fusion communication network is considered, and the rate allocation is optimized based on a heuristic approach that minimizes a weighted sum of communication costs subject to a constraint on the state estimation error at the fusion center. Furthermore, several works tackled the LA for cooperative networks [53]. The authors of [54] propose a Neuro-Fuzzy (NF) algorithm to perform the relay selection and resource allocation process. More recent works (see [55, 56]) tackled the LA problems for multi-source cooperative systems. In [57], a survey is presented related to the LA problem of cooperative networks. We summarize the mentioned LA works in Table 3.

In most of the previously mentioned works, a central node was responsible for the different allocations of resources. Also, in most of the mentioned works the allocation

Table 3 Different link adaptation problems

Link adaptation problem	References
Power allocation	[58, 59]
Cooperative networks power allocation	[46]
Channel allocation	[47, 48, 60, 61]
Cooperative networks channel allocation	[49, 62]
Rate allocation	[50, 63–66]
Rate allocation for cooperative networks	[53–57]

is based on some knowledge of the channel states. Nevertheless, other methods for LA are seen in other frameworks such as game theory (decentralized system) or in learning framework (no knowledge of the channel states). In the learning framework, some of the LA problems can be formulated as multi-armed bandit (MAB) problem. The main issue which MAB framework tackles is the exploration–exploitation dilemma. In scenarios where multiple choices are possible (multiple arms), each with an unknown average reward, MAB algorithms give sequential steps to decide whether we need to learn more (exploration), or to stay with the option that gave the best rewards in the past (exploitation). In the survey [67], three different fundamental types of MAB problems were mentioned, stochastic, adversarial, and Markovian. In UCB-like algorithms, we favor the exploration of actions with a strong potential to have an optimal value [68], and UCB measures this potential by upper confidence bound of the reward value. Thompson sampling (TS) is another type of algorithms widely used [69]. It is quite different to the UCB-type algorithms. The TS algorithms are based on the assumption of posterior distribution for the unknown metric we are trying to learn. The algorithm selects a choice that maximizes its expected reward based on the current distribution. Then, after each iteration, the posterior distribution is updated. In [70], we see a detailed discussion on when, why, and how to apply TS.

Simpler algorithms are also seen in the literature. For example, ϵ -greedy is a well-known algorithm, where a fixed value $\epsilon \in [0, 1]$, decides the percentage of time you spend on exploration and exploitation. Another algorithm is seen in reference [71]. There, rather than using the concept of *optimism in the face of uncertainty*, a new general algorithm that is based on estimation is used. There, the proposal aims at matching the minimal exploration rates of sub-optimal arms as characterized in the derivation of the regret lower bound. We see that some papers (e.g., [72]) compare the previously mentioned algorithms to deduce when each algorithm is favorable.

The MAB framework can be generalized to a case where multiple arms are selected jointly at each decision instance. Such a kind of MAB problem is given under the name of combinatorial MAB (CMAB), where a subset of arms is selected at each step, forming a *Super Arm*. CMAB is seen in different nowadays applications. For example, in [73], beam selection problem is investigated using CMAB algorithms. In [74], combinatorial sleeping MAB model with fairness constraints (CSMAB-F) is presented. The concept of sleeping arm is when some arms are not always available.

In the literature, the LA problem is also seen in decentralized networks. In such networks, the notion of games (and game theory) is presented. In LA games, there are multiple players competing on scarce resources with the goal of getting the optimal reward. The reward of each player is a function of the decision of the player itself and the other competing players. In addition, game theory is seen in cooperative networks such as in interference relay networks [81, 82]. In [80], the problem of joint allocation of power and sub-channel is investigated for cooperative networks. In [80], this problem was tackled using matching theory. There, two low-complexity algorithms are proposed. Another method is to tackle the system using game theory perspective, aiming to study the equilibria points of the system (similar to the analysis presented in [83]). The previous problem can be further separated into two sub-problems, a

sub-channel allocation problem and a power allocation problem. Such separation can lead to a bi-form problem (check for example [86, 87]), i.e., a problem decomposed into a competitive sub-problem (sub-channel allocation) and a cooperative sub-problem (relay power allocation). We summarize the mentioned LA learning and game theory works in Table 4.

1.4 Scope of the paper

In this paper, we aim at studying link adaptation (LA) in the MAMRN, while limiting our study to orthogonal MAMRN, where time division multiplexing (TDM) is used. The simplest way to reduce the effect of interference is to avoid it using orthogonality. From a theoretical information theory point of view, NOMA is known to be more optimal for slow fading channel. Nevertheless, the required complexity of the NOMA receiver design is still not used in practice. On the other hand, other forms of orthogonality such as frequency division multiplexing (FDM) is seen interesting. Accordingly, we presented in our recent work [88] some insights on the generalization of the LA and scheduling strategies when multi-carrier systems are investigated.

As using cooperative systems aims to optimize spectral efficiency, the LA problem is always an open challenge to achieve better spectral efficiency and to satisfy quality of service (QoS) demands. LA is a fundamental mechanism allowing the source nodes to adapt the coding and modulation scheme depending on the radio channel conditions. The destination has to choose a rate for each source from a finite set of rates with the objective to maximize the spectral efficiency. In addition, the system is subject to QoS constraints on individual block error rate (BLER) per source.

In our system, we use centralized LA, where the destination is the center node that determines the source choices. In short, we have a typical multi-variable optimization problem that aims at optimizing the total average spectral efficiency (ASE), subject to QoS constraints. In Fig. 1, we see an illustration of a simple MAMRN. In this figure, we see that all the nodes (sources, relays, and the destination) can listen to each other. Furthermore, we see that there is a link from the destination (the central node) toward the different relaying nodes (sources and relays) representing the feedback information flow. Accordingly, the destination uses these links to share its different decisions and allocations with the different relaying nodes (e.g., allocated rates, selected relaying node, etc.). In other words, the arrows between the sources and the

Table 4 Different link adaptation problems in learning and decentralized networks

Allocation method	References
MAB UCB	[68, 75–77]
MAB TS	[69, 70, 78]
MAB ϵ -greedy	[72]
CMAB	[73, 74, 79]
Matching theory	[80]
Game theory	[81–85]
Bi-form problem	[86, 87]

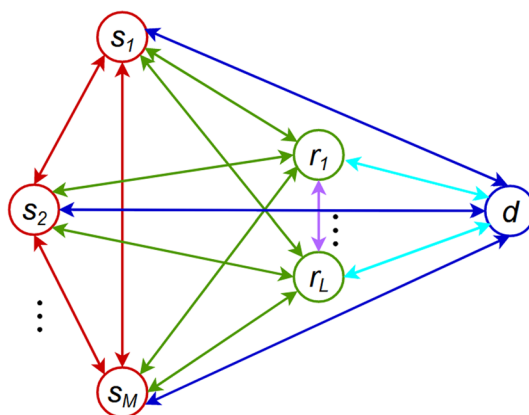


Fig. 1 A MAMRN scheme

relays toward the destination and toward themselves represent the flow of transmitted and retransmitted messages. On the other hand, the arrows from the destination toward the sources and the relays represent the feedback links used by the scheduler at the destination to allocate the resource elements and perform relay selection strategies.

In the literature, in non-cooperative scenarios, where nodes are competing on sparse resources, the best-response dynamics (BRD) appears as a natural approach to solve game-theory problems. In BRD, a player chooses his most favorable outcome taking other players' choices as given. Such tools are seen in several domains [89], especially in decentralized wireless problem, such as rate and power allocation in decentralized cellular networks [90–92]. In our considered problem, and due to the high complexity of its exact solution, we adapt here to the methodology used in the BRD tools trying to give a substantial solution/algorithm to the given centralized multi-variable problem. The main idea is to decrease the complexity of the problem by considering each variable independently while taking the other variables as known information. In our approach, rather than choosing the rates of all the sources at the same time, each source will be handled by the destination successively. Such sequential strategy is sometimes refereed as the Gauss-Seidel procedure (e.g., [93]).

The current authors investigated the problem of rate allocation of the considered system using a multi-armed bandit framework [94]. Although the proposed sequential upper confidence bound 1 (SUCB1) algorithm seems promising, it lacks convergence to the optimal allocation. This is not surprising taking into consideration the cost of exploration that the learning algorithms pay. To avoid this penalty, a LA process can be performed based on the available information at the destination as presented in [95, 96].

In this work, we consider LA for both rate and channel use allocation. In sharp contrast with existing cooperative transmission schemes we consider the packet size to be time-varying. Although this assumption extends the complexity of the allocation problem, it is an interesting degree of freedom which plays an important role in improving the efficiency of the network. The idea is that based on the channel conditions of different sources, it would be better to give more channel uses for a given source in good radio conditions and fewer channel uses for another source in bad radio conditions. Thus, we

propose in this paper low-complexity algorithms that tackle both rate and channel use allocation.

Furthermore, we investigate the performance of these algorithms for both multi-user (MU) encoding and single-user (SU) encoding. The reference [22] investigated different cooperative hybrid automatic repeat reQuest (HARQ) protocols for MAMRN. Nevertheless, no LA algorithms are presented; simply, the comparison of three different HARQ protocols is presented based on a certain rate allocation strategy. To our interest, the authors of [22] tackled both MU encoding and SU encoding, and both schemes gave promising results. While our work is mainly based on the MU encoding where joint network channel coding (JNCC) is used, we analyze as well the performance of our algorithms for the SU encoding sub-case. In MU encoding, a relaying node sends an incremental redundancy (IR)-type of HARQ. This IR signal is representative of all its successfully decoded source messages \mathcal{S} . From both a practical and an information theory viewpoints, the signal sent can help the destination to decode any subset $\mathcal{S}' \subseteq \mathcal{S}$ knowing $\mathcal{S} \setminus \mathcal{S}'$ where \setminus is the minus in set theory. In SU encoding on the contrary, the relaying node chooses (randomly) one source message from its decoding set to retransmit. From a practical point of view, and following the state-of-the-art punctured codes, the SU encoding sub-case is attractive being compatible with codes as low-density parity-check codes or turbo codes.

Finally, two scenarios are investigated:

1. Fast changing radio conditions: where the acquisition of the channel state information (CSI) of all the links is costly in terms of the feedback overhead. Instead, channel distribution information (CDI) (e.g., signal-to-noise ratio (SNR) of the corresponding links) is used in the allocation process, and we call this type of LA slow-link adaptation (SLA). This follows the fact that the initial phase occurs once every few hundred frames, as when the CDI of network links changes. Between two occurrences of the initial phase, the sources' rates are kept fixed. It is called slow in the sense that once a CDI of any link is changed (which occurs every hundreds of frames), the LA is performed. This ensures why such an allocation is practical in fast changing radio conditions (such as in high mobility scenarios).
2. Slow changing radio conditions: where the acquisition of the CSI of all the links is assumed given. This can be practical in scenarios where channel states of all the links change slowly and can be assumed constant during tens of frames. We call this type of LA fast-link adaptation (FLA). It is called fast in the sense that once a CSI of any link is changed (which happens every several frames), the LA is performed. In other words, it is fast adaptation to the changes of the CSI. This ensures why such an allocation is only practical in slow changing radio conditions (as in low mobility scenarios).

In both scenarios, we assume a perfect acquisition of the CSI and the CDI. This means that the information exchange is error-less. In addition, we assume that the overhead of the information acquisition is negligible compared to the frame size. This follows the assumption that the frame size is big enough. We note that the generalization to the case of imperfect information acquisition and small frame size is possible, but several

aspects should be taken into consideration. In such a case, both the rate allocation and the scheduling strategy in the retransmission phase are going to be affected. Indeed, the LA algorithms presented next depend on this information. Accordingly, we will target in a future work the issue of imperfect control exchange process and overhead. The main idea will be to avoid the dependency on the information for the LA strategies.

According to the previous description, we aim to solve the LA problem using a sequential BRD algorithm. The framework we follow next is quite different from the other methods mentioned in the previous subsection such as MAB framework, matching theory, or decentralized game theory solutions. One reason is that we aim to present a solution where there is no need for a penalty for learning. In other words, this paper would act as a benchmark for the different LA algorithms that depend on learning and other frameworks, where the latter frameworks are seen as interesting future work of the considered problem.

Finally, the main contributions of this paper can be summarized as:

- We consider a new degree of freedom by varying the time slot duration of each source in the transmission phase.
- We propose LA algorithms for both slow and fast changing channel conditions scenarios tackling both rate and channel use allocation. The BRD approach is used, with “Genie-Aided” (GA) algorithm for the initialization phase.
- We investigate both MU and SU encoding, showing the efficiency of the practical SU sub-case.
- The numerical results 1- verify the advantages of cooperation, 2- show the gain of exploiting the new degree of freedom (the time slot duration), 3- validate the efficiency of the BRD algorithms for rate and channel use allocation, and finally 4- confirm the efficiency of the practical SU encoding sub-case.

The rest of the paper is organized as follows: in Sect. 2, we introduce the system model. In Sect. 3, we present the mathematical analysis of the used metrics. In Sect. 4, we present the different algorithms of LA using BRD tools. In Sect. 5, we present the Monte-Carlo (MC) simulation results. Finally, we present the conclusions in Sect. 6.

2 System model

The communication system consists of M sources communicating with a single destination, using the help of $M + L$ relaying nodes. The relaying nodes consist of L half-duplex dedicated relays in addition to the M sources, where the latter sources perform user cooperation. A message $\mathbf{u}_s \in \mathbb{F}_2^{K_s}$ of a source s has a length of K_s information bits, where \mathbb{F}_2 represents the binary Galois field. In addition, the length K_s depends on the selected Modulation and Coding Schemes (MCS) for that source. The messages of all sources are mutually independent. To be clear with the notations, we define the source nodes set as $\mathcal{S} = \{1, \dots, M\}$, the relay nodes set as $\mathcal{R} = \{M + 1, \dots, M + L\}$, and all cooperative nodes set as $\mathcal{N} = \mathcal{S} \cup \mathcal{R} = \{1, \dots, M + L\}$. In other words, a source s_i is the node i in set \mathcal{N} , and a relay r_i is the node $i + M$ in set \mathcal{N} .

The transmission of a frame is divided into two phases. A transmission phase is composed of M time slots, where source nodes transmit their messages successively. Then,

we have a retransmission phase composed of several time slots, up to T_{max} time slots. At each retransmission time slot, the scheduler located at the destination schedules one node (source or relay) to transmit redundancies based on its correctly decoded source messages (its decoding set). In the literature, several selection strategies are proposed. In [97] for example, an adaptive relay node selection strategy is proposed based on opportunity. In other words, the destination builds its selection choice following an estimation on the bit error rate (BER).

In the prior art [22], the number of channel uses at each of the transmission phase N_1 and the retransmission phase N_2 was fixed, and accordingly, the ratio of channel uses between the two phases was also fixed. We define this ratio as $\alpha = \frac{N_2}{N_1}$. Here, we introduce a new degree of freedom composed of a variable ratio of the number of channel uses. In particular, we fix the number of channel uses at the retransmission phase, and we define a variable number of channel uses for the transmission phase for each different source node s . In other words, the ratio of channel uses for a source node $s \in \{1, \dots, M\}$ is denoted as $\alpha_s = \frac{N_2}{N_{1,s}}$, where $N_{1,s}$ represents the number of channel uses allocated to source s in the transmission phase.

Following a variable ratio of channel uses, the LA problem gets more complex. In other words, the considered problem of rate allocation is now extended to a problem of rate and channel use allocation. This means that the destination should now allocate the rate and the ratio for each given source node. In Fig. 2, we see an illustration of the frame transmission. A frame consists of three phases: an initialization phase where rates are initialized, a transmission phase where a different number of channel uses is used for each different source node ($N_{1,i}$), and a retransmission phase where a fixed number of channel uses (N_2). A key assumption of our work is that the sources can use packets with variable size at the transmission phase (i.e., $N_{1,i}$ in the first phase), accordingly, the initialization phase includes both rate and channel use allocation. Fixing N_2 and varying N_1 (and not the contrary) is simpler since during the retransmission phase a time slot is not dedicated to a specific node (being a relay or a source).

We retain here the scheduling strategy from [98], which tries to select a node in each time slot of the second phase in a way that maximizes the number of correctly decoded messages at the destination. More precisely, in each retransmission round, the destination selects the node with the highest mutual information between itself and that node, among all nodes which were able to decode at least one source from the set of

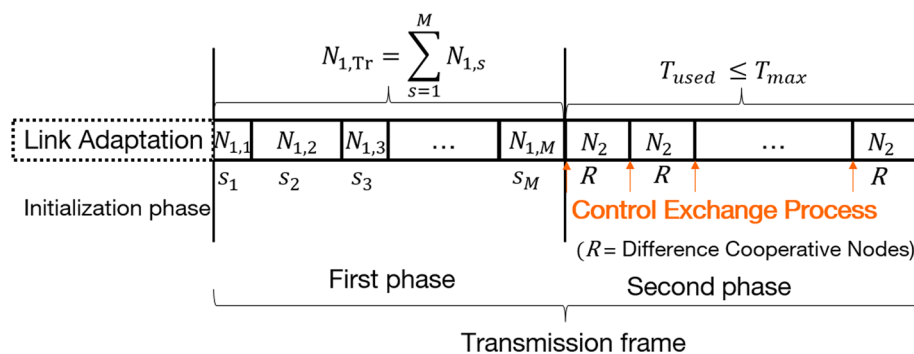


Fig. 2 Proposed frame structure: initialization phase, transmission phase, a retransmission phase

non-successfully decoded sources at the destination. It is demonstrated that using the described strategy, we can reach the ASE close to the upper bound obtained by an exhaustive search for the best possible node activation sequence, under much smaller computational complexity. For that reason, we will only consider the described node selection strategy throughout the whole paper, even though other strategies can be used.

We present in Fig. 3 a toy example that shows how the selection strategy of [98] works. In Fig. 3a, we consider a (3, 2, 1)-MAMRN. At the considered time slot (any time slot in the retransmission phase), the decoding sets of all the nodes are presented. We see that the destination decoded the message of source s_1 , the sources did not decode any source message (but their own message), and the relays r_1 and r_2 decoded respectively the set of sources $\{s_1\}$ and $\{s_1, s_2, s_3\}$. In [98], the candidate relaying nodes to be selected are the nodes that can help at least one source which is not decoded by the destination. As the destination decoded source s_1 , the candidate nodes (in this example) are the relaying nodes that can help either source s_2 or s_3 or both. Following the toy example, the candidate relaying nodes are s_2, s_3 , and r_2 (highlighted in Fig. 3b). After fixing the set of candidate relaying nodes, the destination chooses the node with the highest mutual information. Such a relaying node is the node having the best direct link with the destination. In Fig. 3c, we assume that the best direct link is the link between r_2 and the destination, and thus, r_2 is going to be selected. Finally, in Fig. 3d, we see that r_2 is going to send a symbol representative of all correctly decoded sources which are not decoded yet by the destination, i.e., sources s_2 and s_3 . This process is repeated at the beginning of each retransmission time slot while using the updated decoding sets of the nodes.

Going back to Fig. 2, we see that at each retransmission time slot, a control exchange process is performed. In this process, the relaying nodes give the destination the needed information related to their decoding sets. Then, the destination uses the selection strategy described in the above toy example. More details can be seen in [98] and [16]. From a technical point of view, the presented system model is interesting as it investigates the effects of using relays by allowing for a limited retransmission phase. In [99] for example,

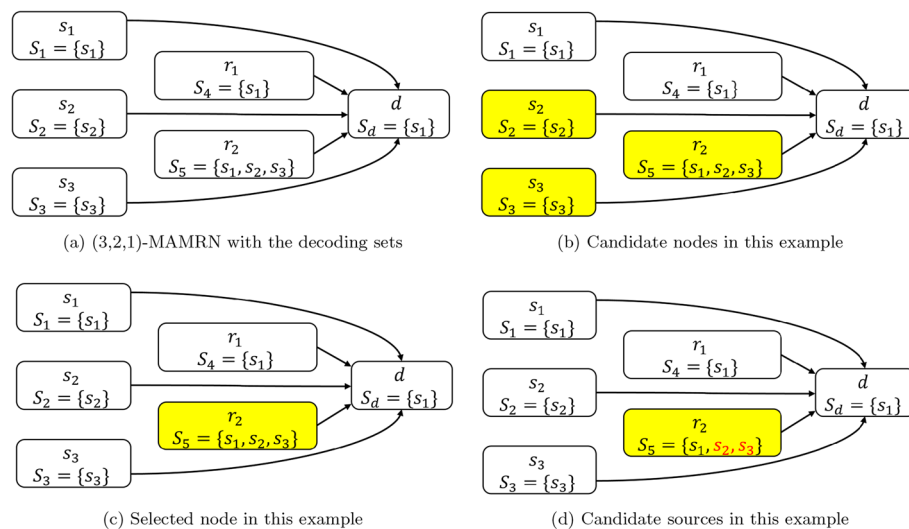


Fig. 3 A toy example describing the process of the selection strategy used in this paper

it is mentioned that the support of multi-path with relay, has a potential to improve the reliability/robustness as well as throughput, so it needs to be considered as an enhancement area in Rel-18. This ensures the modernity and practicality of our targeted system.

We assume a slow fading assumption which means that the radio links between the nodes do not change within a frame transmission. The channel realization is considered independent from frame to frame. It simplifies the analysis and the convergence of the system, and it captures the performance of practical systems assuming ergodicity of the underlying random processes. We assume that the CSI of only the direct links are available at the receiver, i.e., $\mathbf{h}_{\text{dir}} = [\mathbf{h}_{s,d}, \mathbf{h}_{r,d}] = [h_{1,d}, \dots, h_{M+L,d}]$ of Source-to-Destination (S–D), and Relay-to-Destination (R–D) links are perfectly known by the destination. On the other hand, the knowledge of the CSI of other in-direct links, Source-to-Source (S–S), Source-to-Relay (S–R), and Relay-to-Relay (R–R), might not always be possible. Basically, based on the cost of the control overhead, the source and the relay nodes might be able to report the CSI of these in-direct links. In the case where the overhead of reporting the exact CSI is high, the relaying nodes (sources and relays) will only report the CDI of these in-direct links. The overhead is mainly correlated to the mobility of the system, and the destination accordingly chooses which information is reported from the other relaying nodes (CSI or CDI). In Sect. 3, more details will be given. Now, for a given transmitting node $a \in \mathcal{S} \cup \mathcal{R}$, and a receiving node $b \in \mathcal{S} \cup \mathcal{R} \cup \{d\}$, at a given channel use k , the received signal $y_{a,b,k}$ can be written as:

$$y_{a,b,k} = h_{a,b}x_{a,k} + n_{a,b,k}, \tag{1}$$

where $x_{a,k} \in \mathbb{C}$ is the coded modulated symbol whose power is normalized to unity, $h_{a,b}$ are the channel fading gains, which are independent and follow a zero-mean circularly symmetric complex Gaussian distribution with variance $\gamma_{a,b}$, and $n_{a,b,k}$ represents the independent and identically distributed AWGN samples, which follow a zero-mean circularly-symmetric complex Gaussian distribution with unit variance. Note that in the transmission phase, $x_{a,k}$ represents a symbol of a single user. Whereas in the retransmission phase, $x_{a,k}$ represents a symbol representative of all correctly decoded sources by the scheduled relaying node (since JNCC is used).

3 Considered performance metric and outage events

In this Section, we present our utility metric called average spectral efficiency η which is maximized for both FLA and SLA. It is defined as the limit of the ratio between the total number of successfully received bits and the total number of channel uses when the number of frame transmissions tends to infinity. Our analysis relies on the definition of the outage event $\mathcal{O}_{i,t}$ which occurs when source i is not decoded correctly after the transmission phase ($t = 0$) and at each retransmission l up to t ($l = 1, \dots, t$). We define, accordingly, $\mathcal{O}_{i,t}$ as a binary Bernoulli random variable which indicates an outage event. In other words, $\mathcal{O}_{i,t}$ takes the value 1 if the event $\mathcal{O}_{i,t}$ happens, and 0 otherwise. Or, in mathematical terms, for any elementary event w , $\mathcal{O}_{i,t}(w) = [w \in \mathcal{O}_{i,t}]$ where $[q]$ denotes the Inversion bracket which takes the value 1 if q is true, and 0 otherwise. The metric η is derived from the spectral efficiency per frame η^{frame} . η^{frame} depends on the channel realization \mathbf{H} , and the ILA strategy used (strategy of allocating the rate and the channel use of the source nodes) denoted P . Also, it depends on the relaying protocol used,

relaying nodes selection strategy, and the parameters of the system (e.g., $M; L; T_{\max}$). For simplicity, we only include within the following equations the dependency on \mathbf{H} and P . η^{frame} is defined as

$$\begin{aligned} \eta^{\text{frame}}(\mathbf{H}, P) &= \frac{\text{nb bits successfully received}}{\text{nb channel uses}} \\ &= \frac{\sum_{i=1}^M K_i (1 - O_{i, T_{\text{used}}})}{\sum_{l=1}^M N_{1,l} + N_2 T_{\text{used}}} \\ &= \frac{\sum_{i=1}^M \frac{R_i}{\alpha_i} (1 - O_{i, T_{\text{used}}})}{\bar{\alpha} + T_{\text{used}}}, \end{aligned} \tag{2}$$

where:

- \mathbf{H} is the channel realization which contains the channel gains of all the links $h_{a,b}$ previously defined.
- P represents the LA strategy used.
- $\bar{\alpha} = \sum_{i=1}^M 1/\alpha_i$ denotes the sum of inverse of all the channel use ratios,
- $R_i = K_i/N_{1,i}$ represents the rate of a source i ; R_i and α_i have a fixed value for SLA, while they change from frame to frame for FLA,
- $O_{i, T_{\text{used}}}$ is a binary Bernoulli random variable as defined above, i.e., $O_{i, T_{\text{used}}} = 1$ means that source i is not decoded correctly during a frame,
- $T_{\text{used}} \in \{0, \dots, T_{\max}\}$ is the number of retransmission time slots activated during a frame.

The outage indication $O_{i, T_{\text{used}}}$ depends on the knowledge of the CSI of all the links and the sources' rates and ratios. It is obtained from an Information Theory perspective under the classical assumptions of infinite codeword length, mutual information achieving (spatially distributed) channel coding codebooks and maximum likelihood (ML) decoding [100, 101]. The spectral efficiency η can now be derived from η^{frame} .

- For slow-link adaptation: the rates per source and the channel use ratios are fixed, it yields:

$$\eta^{\text{SLA}}(\mathbf{H}, P) = \frac{\sum_{i=1}^M R_i / \alpha_i (1 - \Pr(O_{i, T_{\text{used}}} = 1))}{\bar{\alpha} + \mathbb{E}\{T_{\text{used}}\}}, \tag{3}$$

where $\Pr(O_{i, T_{\text{used}}} = 1)$ is the outage probability that source i is not decoded correctly and $\mathbb{E}\{T_{\text{used}}\}$ is the average number of retransmissions used in the second phase which can be computed as $\mathbb{E}\{T_{\text{used}}\} = \sum_{t=1}^{T_{\max}} t \Pr(T_{\text{used}} = t)$.

- For fast-link adaptation: the rates per source and the channel use ratios change per frame and become random variables, it yields:

$$\eta^{\text{FLA}}(\mathbf{H}, P) = \frac{\mathbb{E}\left\{ \sum_{i=1}^M \frac{R_i}{\alpha_i} (1 - O_{i, T_{\text{used}}}) \right\}}{\mathbb{E}\{\bar{\alpha}\} + \mathbb{E}\{T_{\text{used}}\}}. \tag{4}$$

Note that maximizing the average spectral efficiency as defined above is equivalent to maximizing the average spectral efficiency per frame $\mathbb{E}\{\eta^{\text{frame}}\}$. Indeed, the

maximization of the spectral efficiency of our orthogonal MAMRN protocol is designed in two steps (i) the scheduler at the destination aims at correctly decoding the maximum number of sources with the minimum number of channel uses *per frame* (ii) the LA selects the sources' rates which maximize the average spectral efficiency conditional on the scheduling strategy *per frame*. Finally, since a zero rate can be included in the possible set of rates, and based on the convention that a source with zero rate is always decoded correctly, the two steps above come down to maximizing the average spectral efficiency or the average spectral efficiency per frame conditional on both the considered set of possible discrete rates and the chosen scheduling strategy.

Before presenting the outage events in an analytical way, we recall the effect of the control overhead. From an overhead perspective, SLA is better than FLA as it incurs a smaller overhead. We neglect the overhead of the channel acquisition of the direct links, and we focus on the overhead of the in-direct links which is the most costly. In a given $(M, L, 1)$ -MAMRN, the number of the in-direct links corresponds to the number of possibilities to select two nodes among $M + L$ which is C_2^{M+L} where C is the combination operator. This means that the overhead can be calculated as $C_2^{M+L} \times \text{nb bits per CSI/CDI} \times \text{update percentage}$. Accordingly, it is obvious that unless the percentage of change in the CSI is low, we have to adapt to the SLA as the percentage of change in the CDI is usually very small (the CDI is fixed for a long time, e.g., 1000 frames: 0.1%)

Now, we present the outage events of the system which are the individual outage event for a given source, and the common outage event for a subset of sources. The latter occurs when at least one user in the subset of sources is in outage. In [18], Mohamad et al provide an outage analysis for various cooperative schemes. Nevertheless, the analysis was based on a fixed channel uses in the transmission phase. Accordingly, we present here the outage derivations when the number of channel uses in the transmission phase is considered variable. In general, the "individual outage event of a source s after round t ", $\mathcal{O}_{s,t}(a_t, \mathcal{S}_{a_t,t-1} | \mathbf{h}_{\text{dir}}, \mathcal{P}_{t-1})$, depends directly on the rate and channel uses we are scheduling. In addition, it depends on the selected node $a_t \in \mathcal{N}$ and its associated decoding set $\mathcal{S}_{a_t,t-1}$. It is conditional on the knowledge of \mathbf{h}_{dir} and \mathcal{P}_{t-1} , where \mathcal{P}_{t-1} denotes the set collecting the nodes \hat{a}_l which were selected in rounds $l \in \{1, \dots, t-1\}$ prior to round t together with their associated decoding sets $\mathcal{S}_{\hat{a}_l,l-1}$, and the decoding set of the destination $\mathcal{S}_{d,t-1}$ ($\mathcal{S}_{d,0}$ is the destination's decoding set after the first phase).

Similarly, we define $\mathcal{E}_t(a_t, \mathcal{S}_{a_t,t-1} | \mathbf{h}_{\text{dir}}, \mathcal{P}_{t-1})$ the "common outage event after round t " as the event that at least one source is not decoded correctly at the destination at the end of round t . The probability of the individual outage event of source s after round t , $\Pr(\mathcal{O}_{s,t}(a_t, \mathcal{S}_{a_t,t-1} | \mathbf{h}_{\text{dir}}, \mathcal{P}_{t-1}) = 1)$, for a candidate node a_t using the expectation operator $\mathbb{E}\{\cdot\}$ can be formulated as $\mathbb{E}\{\mathcal{O}_{s,t}(a_t, \mathcal{S}_{a_t,t-1} | \mathbf{h}_{\text{dir}}, \mathcal{P}_{t-1})\}$. We can similarly define the probability of the common outage event. In the rest of the paper, and in order to simplify the notation, the dependency on \mathbf{h}_{dir} and \mathcal{P}_{t-1} is omitted.

Analytically, the common outage event of a given subset of sources is declared if the vector of their rates lies outside the corresponding MAC capacity region. We recall that although this is an orthogonal transmission framework, the outage events encounter the interference effects. Clearly, this follows the JNCC used, where a re-transmitted message can include information about different source messages. Now, for some subset

of sources $\mathcal{B} \subseteq \overline{\mathcal{S}}_{d,t-1}$, where $\overline{\mathcal{S}}_{d,t-1} = \mathcal{S} \setminus \mathcal{S}_{d,t-1}$ is the set of non-successfully decoded sources at the destination after round $t - 1$, and for a candidate node a_t , this event can be expressed as:

$$\begin{aligned} \mathcal{E}_{t,\mathcal{B}}(a_t, \mathcal{S}_{a_t,t-1}) &= \bigcup_{\mathcal{U} \subseteq \mathcal{B}} \left\{ \sum_{i \in \mathcal{U}} \frac{R_i}{\alpha_i} > \sum_{i \in \mathcal{U}} \frac{I_{i,d}}{\alpha_i} + \sum_{l=1}^{t-1} I_{\hat{a}_l,d} \mathcal{C}_{\hat{a}_l}(\mathcal{U}) + I_{a_t,d} \mathcal{C}_{a_t}(\mathcal{U}) \right\}, \end{aligned} \tag{5}$$

where $I_{a,b}$ denotes the mutual information between the nodes a and b (the mutual information is defined based on the channel inputs, check Sect. 5 for Gaussian inputs example), and where $\mathcal{C}_{\hat{a}_l}$ and \mathcal{C}_{a_t} have the following definitions:

$$\begin{aligned} \mathcal{C}_{\hat{a}_l}(\mathcal{U}) &= \left[(\mathcal{S}_{\hat{a}_l,l-1} \cap \mathcal{U} \neq \emptyset) \wedge (\mathcal{S}_{\hat{a}_l,l-1} \cap \mathcal{I} = \emptyset) \right], \\ \mathcal{C}_{a_t}(\mathcal{U}) &= \left[(\mathcal{S}_{a_t,t-1} \cap \mathcal{U} \neq \emptyset) \wedge (\mathcal{S}_{a_t,t-1} \cap \mathcal{I} = \emptyset) \right]. \end{aligned} \tag{6}$$

In (6), the sources that belong to $\mathcal{I} = \overline{\mathcal{S}}_{d,t-1} \setminus \mathcal{B}$ are considered as interference, with \wedge standing for the logical and. In (5), for each subset \mathcal{U} of set \mathcal{B} , we check if the sum-rate of sources contained in \mathcal{U} is higher than the accumulated mutual information at the destination (since Incremental Redundancy (IR)-type of HARQ is used). The accumulated mutual information is split into three summations, which originate from:

- The direct transmissions from sources contained in \mathcal{U} toward the destination during the first phase: $\sum_{i \in \mathcal{U}} \frac{I_{i,d}}{\alpha_i}$.
- The transmission of previously activated nodes during the second phase: $\sum_{l=1}^{t-1} I_{\hat{a}_l,d} \mathcal{C}_{\hat{a}_l}(\mathcal{U})$. Node \hat{a}_l for $l = \{1, \dots, t - 1\}$ is involved in the calculation only if it was able to successfully decode at least one source from the subset \mathcal{U} (JNCC is used), but at the same time, if it does not belong to the set \mathcal{I} (otherwise, the signal would represent an interference).
- The transmission of the candidate node a_t during the second phase: $I_{a_t,d} \mathcal{C}_{a_t}(\mathcal{U})$, under the same conditions as for the previously activated nodes.

The individual outage event of a source s after round t for a candidate node a_t can be defined as:

$$\begin{aligned} \mathcal{O}_{s,t}(a_t, \mathcal{S}_{a_t,t-1}) &= \bigcap_{\mathcal{I} \subseteq \overline{\mathcal{S}}_{d,t-1}, \mathcal{B} = \overline{\mathcal{I}}, s \in \mathcal{B}} \mathcal{E}_{t,\mathcal{B}}(a_t, \mathcal{S}_{a_t,t-1}), \\ &= \bigcap_{\mathcal{I} \subseteq \overline{\mathcal{S}}_{d,t-1}} \bigcup_{\mathcal{U} \subseteq \overline{\mathcal{I}}: s \in \mathcal{U}} \left\{ \sum_{i \in \mathcal{U}} \frac{R_i}{\alpha_i} > \sum_{i \in \mathcal{U}} \frac{I_{i,d}}{\alpha_i} + \sum_{l=1}^{t-1} I_{\hat{a}_l,d} \mathcal{C}_{\hat{a}_l}(\mathcal{U}) + I_{a_t,d} \mathcal{C}_{a_t}(\mathcal{U}) \right\}, \end{aligned} \tag{7}$$

where $\overline{\mathcal{I}} = \overline{\mathcal{S}}_{d,t-1} \setminus \mathcal{I}$. The detailed analysis behind the relation between the individual outage event and the common outage event can be revisited in [18].

We finally define the outage events equations for the SU encoding sub-case. Since the relaying node transmits redundancies of a single source (which is chosen

randomly from its decoding set), the individual outage event of a source s after round t for a candidate node a_t can be written as:

$$\mathcal{O}_{s,t}^{SU}(a_t, \mathcal{S}_{a_t,t-1}) = \left\{ \frac{R_i}{\alpha_i} > \frac{I_{i,d}}{\alpha_i} + \sum_{l=1}^{t-1} I_{\hat{a}_l,d} C_{\hat{a}_l}^{SU} + I_{a_t,d} C_{a_t}^{SU} \right\}, \tag{8}$$

where $C_{\hat{a}_l}^{SU}$ (respectively $C_{a_t}^{SU}$) takes the value 1 if the source s is chosen by \hat{a}_l (respectively a_t) and zero otherwise. For the common outage event, in the SU encoding sub-case, it is simply the union of the individual outage events of all the sources included in the considered subset \mathcal{B} , and can be written as:

$$\mathcal{E}_{t,\mathcal{B}}^{SU}(a_t, \mathcal{S}_{a_t,t-1}) = \bigcup_{s \in \mathcal{B}} \mathcal{O}_{s,t}^{SU}(a_t, \mathcal{S}_{a_t,t-1}). \tag{9}$$

4 Methods: proposed link adaptation strategy

In MAMRN, the knowledge of instantaneous CSI of all the links allows the LA algorithm to allocate the rates and the ratios of the sources in the most accurate way (fast-link adaptation). Since the number of channels in such a network grows exponentially with the number of sources and relays, frequent changes in the channel states (for ex. in a high mobility scenario) can incur an excessive amount of control signaling on the forward coordination control channels. In that case, FLA is deemed impractical, and SLA is a more suitable solution. The idea of SLA is to adapt the source rates to the CDI of all links, which remain constant for longer periods of time. It is important to stress that the time-scale of the SLA differs from the one used by the retransmission algorithm.

Following the considered orthogonal MAMRN system model, the individual outage event (resp. the probability of outage event) of any node depends on the vector of rates and ratios allocated for all the source nodes considered in the system. In other words, $\mathcal{O}_{s,T_{\max}}$ (resp. $\Pr(\mathcal{O}_{s,T_{\max}})$) depends on the vector of pairs $(\{R_1, \alpha_1\}, \dots, \{R_M, \alpha_M\})$. To understand this dependency, we should be aware that at a given retransmission time slot, the decoding set of the selected node to retransmit, depends on all the rates and ratios allocated. Also, with a small observation of the analytical definition of the individual outage event, i.e., Eq. (7), we see that theoretically, the vector of pairs should be jointly optimized.

Before we present the optimization problem, we define the corresponding notations:

- n_{MCS} is the number of different modulation and coding schemes available.
- $\{\tilde{R}_1, \dots, \tilde{R}_{n_{\text{MCS}}}\}$ is the set of possible rates available.
- n_{CUR} is the number of different channel use ratios (CUR) available.
- $\{\tilde{\alpha}_1, \dots, \tilde{\alpha}_{n_{\text{CUR}}}\}$ is the set of possible channel use ratios available.
- $\{\tilde{R}_s, \tilde{\alpha}_s\}$, is the pair of rate and channel use ratio of source s after the optimization.
- R_i , one possible value of \tilde{R}_s taken from the set of possible rates available.
- α_i , one possible value of $\tilde{\alpha}_s$ taken from the set of possible channel use ratios available.

Using these notations, our given optimization problem can be written as:

$$\begin{aligned}
 & (\{\hat{R}_1, \hat{\alpha}_1\}, \dots, \{\hat{R}_M, \hat{\alpha}_M\}) = \\
 & \quad \text{argmax} \\
 & \quad (\{R_1, \alpha_1\}, \dots, \{R_M, \alpha_M\}) \in \{\{\hat{R}_1, \hat{\alpha}_1\}, \dots, \{\hat{R}_{n_{MCS}}, \hat{\alpha}_{n_{CUR}}\}\}^M \\
 & \quad \frac{\sum_{i=1}^M R_i / \alpha_i (1 - \Pr(O_{i, T_{used}} = 1))}{\bar{\alpha} + \mathbb{E}\{T_{used}\}}, \tag{10} \\
 & \text{subject to:} \\
 & \Pr(O_{i, T_{used}} = 1) \leq BLER_{QoS, i}, \forall i \in \{1, \dots, M\}, \\
 & R_i \geq R_{min, i}, \forall i \in \{1, \dots, M\}.
 \end{aligned}$$

This equation corresponds to the SLA scenario. Obviously, in the case of FLA, we replace $\Pr(O_{i, T_{used}} = 1)$ with $O_{i, T_{used}}$ and $\mathbb{E}\{T_{used}\}$ with T_{used} , since LA is performed for each new instance of the channels. In SLA, a QoS constraint *per source* is introduced as a minimum rate with an outage probability threshold (BLER). For FLA, since the full CSI is known at the destination, it is possible to avoid any individual outage per frame by simply not transmitting or, equivalently, transmitting with zero rate. Furthermore, we chose not to introduce any constraint on minimum rates in order to have a benchmark on the maximum achievable spectral efficiency.

To our knowledge, a closed-form solution for this multi-variable optimization problem is not found yet. Indeed, there is always the possibility to find the solution to such a problem by checking exhaustively all $(n_{MCS} \times n_{CUR})^M$ possible combinations of allocated rates and ratios, and choosing the one which maximizes the ASE subject to individual QoS constraints. Clearly, such an approach is computationally very expensive. Accordingly, sub-optimal solutions are needed to relax the complexity of the problem, and thus we resort to BRD tools.

Following the BRD approach, the problem is solved in two steps: in step one, the destination chooses the initial source rates and ratios, then in step two, the destination uses the BRD methods to update the initial allocations by searching for a better result. The correction is done iteratively for each source node (not jointly), and the correction process is repeated until convergence to the “optimal” solution is reached. As compared to the prior art [95], our added contribution is that we generalize the BRD algorithm to capture both rate and channel use allocation. In addition, we present in detail the starting point strategy used and which was omitted in the prior-art. In the following subsection, we attempt to find a clever algorithm to reach a good starting point, since the optimal solution and the convergence speed will depend on it. Thus, rather than using random source rates values, we follow a GA assumption and try to find a suitable initialization algorithm.

4.1 Starting point using the “Genie-Aided” assumption

In order to reduce the complexity, we can resort to an approach that is based on a “Genie-Aided” assumption, where all the sources $s \in \mathcal{S} \setminus i = \{1, 2, \dots, i - 1, i + 1, \dots, M\}$ except the one for which we want to allocate the rate and the ratio, i , are assumed to be decoded correctly at the destination and the relaying nodes. Concerning the ratio, we see that even in that case, we still have a dependency on all the other source nodes’ ratios. This is due to the summation seen in the denominator of Eq. (10) (the number

of total channel uses of the transmission phase). In other words, in order to decouple the problem, the ratios of channel uses are fixed to a certain value first (we resort here to the average value of all the possible ratios $A = \{\tilde{\alpha}_1, \dots, \tilde{\alpha}_{n_{CUR}}\}$). Then, the rate of each source node is allocated from the set of possible rates $\{\tilde{R}_1, \dots, \tilde{R}_{n_{MCS}}\}$.

Using the GA relaxation, the problem gets less complex. In other words, the rate selection of a given source becomes independent of the selection of another source. This is done by avoiding the dependency on the decoding sets of the different relaying nodes. From a viewpoint of a source i , the MAMRN reduces to $(1, L + M - 1, 1)$ multiple relay network. In addition, the problem of allocating a {rate, ratio} pair is reduced to only rate allocation. An example is given in Fig. 4 for $i = s_1$, where the sources $\{s_2, \dots, s_M\}$ are symbolically denoted by $\{r_{L+1}, \dots, r_{L+M-1}\}$, as they only serve as relays. Under the GA assumption, the node selection strategy will give a different sequence of selected nodes than the case where the GA assumption is not taken. This follows the fact that under the GA assumption, the source i is the only one that is not decoded correctly at the destination. Thus, all the scheduling decisions are oriented toward helping this source exclusively, which results in an allocated rate higher than the optimal one. Possibly a better approximation of the realistic node selection sequence while evaluating rate R_i in the GA algorithm, is a random node activation sequence, and that approach is adopted in the rest of the paper when using GA.

Hence, although the initial rates found under the GA assumption are not the exact solutions of the maximization problem (10), they can serve as a good starting point for finding the optimal solutions. Indeed, even though we always consider that only one source is not decoded correctly, which is not a realistic assumption, and that the node activation sequence is purely random, we take into account the quality of all the links which can potentially help the transmission of a given source in the calculation.

In this paper, in the SLA scenario, we assume that the channel statistics of each link follows a centered circularly complex Gaussian distribution. Since the links are independent of each other, the average SNR of each link is sufficient as an input to trace back the statistics of each link. Given the simplified, $(1, L + M - 1, 1)$ network, the problem of finding the maximum rate R_s for the source s subject to a $BLER_{QoS,s}$ constraint has the following form:

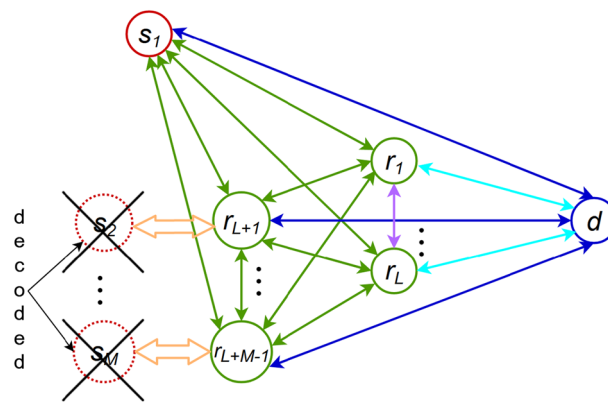


Fig. 4 Illustration of the "Genie-Aided" assumption

$$\begin{aligned} \widehat{R}_s^{\text{SLA}} &= \operatorname{argmax}_{R_i \in \{\widetilde{R}_1, \dots, \widetilde{R}_{n_{\text{MCS}}}\}} \left\{ \frac{R_i(1 - \Pr(\text{O}_{i,T_{\text{used}}} = 1))}{M + \alpha \mathbb{E}\{T_{\text{used}}\}} \right\} \\ &\text{subject to } \Pr\{\text{O}_{s,T_{\text{used}}} = 1\} \leq \text{BLER}_{\text{QoS},s}, \\ &\text{and } R_i \geq R_{\min,s}, \end{aligned} \tag{11}$$

where $\Pr(\text{O}_{i,T_{\text{used}}} = 1)$ can be written as:

$$\begin{aligned} \Pr(\text{O}_{i,T_{\text{used}}} = 1) &= \int \left[R_i > I_{s,d} + \sum_{l=1}^{T_{\text{used}}} \alpha I_{\widehat{a}_l,d}[s \in \mathcal{S}_{\widehat{a}_l,l-1}] \right] P(\mathbf{H}) d\mathbf{H}, \end{aligned} \tag{12}$$

with $P(\mathbf{H})$ is the joint probability of channel realizations of all the links in the network, and α is the fixed average value of the ratios. Note that Eq. (11) is reached after a direct simplification of Eq. (10). Simply, only one source node is considered, and all α_i are fixed to α . The problem of finding the maximum rate R_s for source s in the case of FLA simplifies to the following:

$$\begin{aligned} \widehat{R}_s^{\text{FLA}} &= \operatorname{argmax}_{R_i \in \{\widetilde{R}_1, \dots, \widetilde{R}_{n_{\text{MCS}}}\}} \left\{ \frac{R_i}{M + \alpha T_{\text{used}}} \left(1 - \left[R_i > I_{s,d} + \sum_{l=1}^{T_{\text{max}}} \alpha I_{\widehat{a}_l,d}[s \in \mathcal{S}_{\widehat{a}_l,l-1}] \right] \right) \right\}. \end{aligned} \tag{13}$$

A detailed step-by-step algorithm in which a rate is allocated to source i under GA assumption with CDI available at the destination (SLA) is given by algorithm 1. First, we set the initial best efficiency, and then we set α as the ratio that is closest to the average ratio. Then, each possible candidate rate from the set $\{\widetilde{R}_1, \dots, \widetilde{R}_{n_{\text{MCS}}}\}$ is considered one after another in the first “for loop” on j . We only consider the rates satisfying the minimum rate constraint $R_j \geq R_{\min,j}$. The second “for loop” allows to average out the $\Pr(\text{O}_{i,T_{\text{used}}} = 1)$, for the given rate R_j over Nb_MC realizations of all channels. The averaging is done according to statistics given by the average SNRs of all links. Hence, inside the loop cnt , the quality of each channel is known, since they result from the random realization of all channels. Therefore, in order to calculate (11), it is sufficient to use the Monte-Carlo simulations approach, where the integral in Eq. (12) is replaced by a sum, and thus, Eq. (12) can be computed by:

$$\begin{aligned} \Pr(\text{O}_{i,T_{\text{used}}} = 1) &= \frac{1}{\text{Nb_MC}} \sum_{cnt=1}^{\text{Nb_MC}} \left[R_i > I_{i,d}(\mathbf{H}_{cnt}) + \sum_{l=1}^{T_{\text{max}}} \alpha I_{\widehat{a}_l,d}(\mathbf{H}_{cnt})[i \in \mathcal{S}_{\widehat{a}_l,l-1}] \right]. \end{aligned} \tag{14}$$

Algorithm 1 Slow-link adaptation algorithm based on “Genie-Aided” assumption for source i s.t. $BLE_{QoS,i}$ target.

```

1:  $S_{best} \leftarrow -1.$  ▷ Initialize the best efficiency to -1.
2:  $\alpha_{average} \leftarrow \frac{1}{|A|} \sum_{q=1}^{|A|} \tilde{\alpha}_q$  where  $A = \{\tilde{\alpha}_1, \dots, \tilde{\alpha}_{CUR}\}.$ 
3:  $\alpha \leftarrow \underset{\tilde{\alpha} \in A}{\operatorname{argmin}} |\tilde{\alpha} - \alpha_{average}|.$  ▷ Choose ratio closest to the average
4: for  $j \leftarrow 1$  to  $n_{MCS}$  do ▷ Number of candidate rates.
5:   Pick sequentially  $R_j \in \{\tilde{R}_1, \dots, \tilde{R}_{n_{MCS}}\}$  s.t.  $R_j \geq R_{min,j}.$ 
6:    $out \leftarrow 0.$  ▷ Counter of MC samples leading to outage.
7:    $\bar{T}_{used} \leftarrow 0.$  ▷ Accumulated nb. of rounds used in the 2. phase.
8:   for  $cnt \leftarrow 1$  to  $Nb\_MC$  do ▷ Max. number of MC samples
9:     Draw  $\mathbf{H}_{cnt}$  based on  $P(\mathbf{H}).$ 
10:    Calculate  $I_{a,b}(\mathbf{H}_{cnt})$  for  $\forall a \in N, \forall b \in \{N \cup \{d\} \setminus \{a\}\}.$ 
11:    if  $R_j \leq I_{i,d}$  then
12:       $S_{d,0} \leftarrow S_{d,0} \cup \{i\}.$ 
13:      continue. ▷  $out$  and  $\bar{T}_{used}$  do not change.
14:    end if
15:    for  $t \leftarrow 1$  to  $T_{max}$  do ▷ For each round we do:
16:      Random node selection by the scheduler:  $\hat{a}_t.$ 
17:       $C_1 \leftarrow I_{i,\hat{a}_t} + \sum_{k=1}^{t-1} \alpha I_{\hat{a}_k,\hat{a}_t} \mathbf{1}_{\{i \in S_{\hat{a}_k,k-1}\}}.$  ▷ Acc.
18:      mut. inf. between  $i$  and  $\hat{a}_t.$ 
19:      if  $R_j \leq C_1$  then ▷ Check if  $\hat{a}_t$  has decoded  $i.$ 
20:         $S_{\hat{a}_t,t-1} \leftarrow S_{\hat{a}_t,t-1} \cup \{i\}.$ 
21:      end if
22:       $C_2 \leftarrow I_{i,d} + \sum_{k=1}^t \alpha I_{\hat{a}_k,d} \mathbf{1}_{\{i \in S_{\hat{a}_k,k-1}\}}.$ 
23:      if  $R_j \leq C_2$  then ▷ Check if the dest. has decoded  $i.$ 
24:         $S_{d,t} \leftarrow S_{d,t} \cup \{i\}.$ 
25:         $T_{used} \leftarrow t.$  ▷ Nb. of rounds used for the current MC sample.
26:      break. ▷  $out$  does not change.
27:    end if
28:    if  $t = T$  then
29:       $out \leftarrow out + 1.$ 
30:       $T_{used} \leftarrow T.$ 
31:    end if
32:  end for
33:   $\bar{T}_{used} \leftarrow \bar{T}_{used} + T_{used}.$ 
34:   $P_{i,R_j}^{out} \leftarrow \frac{out}{Nb\_MC}$  ▷ The avg. outage prob. of  $i$  with  $R_j.$ 
35:   $\mathbb{E}\{T_{used,R_j}\} \leftarrow \frac{\bar{T}_{used}}{Nb\_MC}$  ▷ The avg. nb. of rounds used in the 2. phase.
36:   $S \leftarrow \left\{ \frac{R_j}{M + \alpha \mathbb{E}\{T_{used,R_j}\}} \left( 1 - P_{i,R_j}^{out} \right) \right\}$  ▷ Compute the current efficiency.
37:  if  $S > S_{best}$  and  $P_{i,R_j}^{out} \leq BLE_{QoS,i}$  then
38:     $S_{best} \leftarrow S$  and  $R_{best} \leftarrow R_j$ 
39:  end if
40: end for
41:  $\hat{R}_i \leftarrow R_{best}$ 

```

The FLA algorithm is very similar to the SLA one, so it is left out of the text. The main difference is the absence of the averaging of the individual outage probability over Nb_MC realizations of all channels. For that reason, variables out , \bar{T} , P_{i,R_j}^{out} and $\mathbb{E}\{T_{used,R_j}\}$ are not used, nor is the “for” loop on cnt . Additionally, instead of drawing

the channels \mathbf{H}_{cnt} , it is assumed that \mathbf{H} is already known at the destination due to available CSI information of all channels.

4.2 Sequential best-response dynamic solution

After setting up the starting point of the rates and the ratios (rates using GA and ratios using an average value), the BRD algorithm follows. The idea is to modify, iteratively, the chosen rates and ratios. Since the joint allocation is very complex, we will correct the starting point chosen for each source node successively. In that case, the rate and the ratio of source i is a function of the sources' rates and ratios updated in the same iteration prior to source i (sources with index $i' < i$), and the rates and ratios updated for the last time in the previous iteration, $t - 1$ (sources with index $i'' > i$). The logic is repeated until the algorithm converges when no source node modifies its rate or ratio any further.

In the correction method described above, a given source i chooses the best rate-ratio pair corresponding to the maximum spectral efficiency while meeting the QoS constraints. Based again on Eq. (10), we write the optimization problem for a given source node i as:

$$\begin{aligned} \{\hat{R}_i, \hat{\alpha}_i\} = & \operatorname{argmax}_{\{R_i, \alpha_i\} \in \{\{\hat{R}_1, \hat{\alpha}_1\}, \dots, \{\hat{R}_{n_{MCS}}, \hat{\alpha}_{n_{CUR}}\}\}} \\ & \frac{\sum_{j=1, j \neq i}^M \frac{\hat{R}_j}{\hat{\alpha}_j} (1 - \Pr(O_{j, T_{used}} = 1)) + \frac{R_i}{\alpha_i} (1 - \Pr(O_{i, T_{used}} = 1))}{\bar{\alpha} + \mathbb{E}\{T_{used}\}}, \end{aligned} \tag{15}$$

subject to:

$$\Pr(O_{s, T_{used}} = 1) \leq BLER_{QoS, s}, \forall s \in \{1, \dots, M\},$$

$$\text{and } R_i \geq R_{\min, i}.$$

Algorithm 2 Best-Response algorithm under the QoS constraints on individual BLER targets $BLER_{QoS, i}, \forall i \in \{1, \dots, M\}$.

- 1: $t \leftarrow 0$. ▷ Counter of iterations.
 - 2: Set the candidate rates and ratios: $\{\hat{R}_1, \dots, \hat{R}_{n_{MCS}}\}, \{\hat{\alpha}_1, \dots, \hat{\alpha}_{n_{CUR}}\}$.
 - 3: Rate and Ratio initialization under GA assumption with a random node selection:
 $[\hat{R}_1(0), \dots, \hat{R}_M(0)] \leftarrow [R_1^{GA}, \dots, R_M^{GA}]$,
 $[\hat{\alpha}_1(0), \dots, \hat{\alpha}_M(0)] \leftarrow [\alpha_1^{GA}, \dots, \alpha_M^{GA}]$.
 - 4: $\{\hat{R}_i(-1), \hat{\alpha}_i(-1)\} \leftarrow \{0, 0\}$ for all $i \in \{1, \dots, M\}$ ▷ To force loop to start
 - 5: **while** $(|\hat{R}_i(t) - \hat{R}_i(t-1)| > 0 \text{ or } |\hat{\alpha}_i(t) - \hat{\alpha}_i(t-1)| > 0)$, for some $i \in \{1, \dots, M\}$ **do**
 - 6: $t \leftarrow t + 1$.
 - 7: **for** $i \leftarrow 1$ **to** M **do** ▷ for all sources, choose:
 - 8: $\{\hat{R}_i(t), \hat{\alpha}_i(t)\} \leftarrow$
 $\operatorname{argmax}_{\{R_i, \alpha_i\} \in \{\{\hat{R}_1, \hat{\alpha}_1\}, \dots, \{\hat{R}_{n_{MCS}}, \hat{\alpha}_{n_{CUR}}\}\}}$
 $\eta(\{\hat{R}_1(t), \hat{\alpha}_1(t)\}, \dots, \{\hat{R}_{i-1}(t), \hat{\alpha}_{i-1}(t)\}, \{R_i, \alpha_i\},$
 $\{\hat{R}_{i+1}(t-1), \hat{\alpha}_{i+1}(t-1)\}, \dots, \{\hat{R}_M(t-1), \hat{\alpha}_M(t-1)\})$
▷ the pair which maximizes η
such that $\Pr\{O_{s, T_{used}} = 1\} \leq BLER_{QoS, s}, \forall s \in S$
and $R_i \geq R_{\min, i}$
▷ while satisfying the constraints
 - 9: **end for**
 - 10: **end while**
-

Algorithm 2 presents the BRD algorithm in the case of the SLA scenario. The same modifications mentioned in the algorithm of the GA approach are needed here to adapt to the algorithm of the FLA. The destination first initializes the rates and ratios following the result of the GA approach, and then it performs the correction process for all the M source nodes. The algorithm terminates once we have no further changes in the rate and ratio choices for all the source nodes. A small remark should be mentioned about step 8 of the BRD algorithm. By this step, we have captured all the details previously mentioned in the GA algorithm (between step 8 and step 33), i.e., the details of the Monte-Carlo simulation used to obtain the outage probability and the average number of rounds used. This is done for the sake of brevity, but both algorithms do individual outage tests to achieve the QoS constraint while allocating the rates and the ratios.

By performing Monte-Carlo simulations, where the results are presented in the following Section, we witness that the number of iterations needed for the algorithm to converge is relatively small. In addition, we witness that the Monte-Carlo method is robust to the number of samples, as the degradation seen with decreasing the number of samples is not significant, i.e., the results barely change even when simulations were based on only 10 samples. Moreover, we have demonstrated that the utility function is not always convex since the BRD, when initialized with other starting points than the GA, can converge to a local optimum far from the global one depending on the simulation scenario (not presented for brevity). It confirms that the convergence analysis is simulation scenario dependent, which makes it extremely difficult to tackle analytically. In the next subsection, we talk about the convergence and the complexity of the BRD algorithm used.

4.3 Convergence and complexity

Convergence:

Theorem 1 *The BRD algorithm converges to an optimal (local or global) rate and ratio allocation after a limited number of iterations.*

Proof: The BRD is composed of an initialization step and an iterative correction step. The initialization step is always fixed to 1 iteration. Concerning the correction step, it lasts till we reach the stopping condition (step 5 in algorithm 2). We call the number of BRD iterations n_{BRD} and the number of correction iterations as n_{corr} . The number of BRD iterations can be written as:

$$n_{\text{BRD}} = 1 + n_{\text{corr}}. \quad (16)$$

To prove that the BRD algorithm converges in a finite number of iteration, we see that the stopping condition happens when the allocation of all the sources' rates and ratios is not changed from the previous iteration for all sources $i \in \{1, \dots, M\}$. Since the number of possible rate and ratio pairs for the M sources is finite $((n_{\text{MCS}} \times n_{\text{CUR}})^M)$, and since the *argmax* at step 8 only updates the rates and ratios if η strictly increases, we deduce that

Table 5 Different allocation methods with their corresponding complexities and performance

Allocation method	Complexity	Properties
Exhaustive with variable α	$\Omega((n_{MCS} \times n_{CUR})^M)$	Optimal but complex: exponential with M and linear with n_{MCS} and n_{CUR}
Exhaustive with fixed α	$\Omega((n_{MCS})^M)$	Optimal (for fixed α) but complex: exponential with M and linear with n_{MCS}
BRD with variable α	$\Omega(n_{MCS} \times n_{CUR} \times M \times n_{BRD})$	Approaches the exhaustive method with lower complexity (linear with M)
BRD with fixed α	$\Omega(n_{MCS} \times M \times n_{BRD})$	Approaches the exhaustive method (for fixed α) with lower complexity (linear with M)
GA with variable α	$\Omega(n_{MCS} \times n_{CUR} \times M)$	Low complexity but with mediocre performance
GA with fixed α	$\Omega(n_{MCS} \times M)$	Low complexity but with mediocre performance
Fixed allocation	$\Omega(1)$	Unacceptable performance

$$n_{corr} \leq (n_{MCS} \times n_{CUR})^M - 1, \tag{17}$$

leading to the final result of

$$n_{BRD} \leq (n_{MCS} \times n_{CUR})^M, \tag{18}$$

where the latter inequality goes to equality in the worst-case scenario that rarely occurs as seen in the numerical results in the following Section. We conclude that the process of BRD completes with a finite number of iterations.

Although the BRD algorithm converges in finite number of iterations, the speed of convergence is a function of this number (i.e., n_{BRD}). Due to this issue, we investigated in the next Section the number of iterations needed before convergence, and we see that this number is relatively small, validating the practicality of the proposed solution.

Complexity:

The complexity of the proposed BRD algorithm is much smaller than the case of the exhaustive search approach algorithm. In the latter, the calculation of each $\Pr(O_{i,T_{used}} = 1)$ is performed $(n_{MCS} \times n_{CUR})^M$ times, while in the proposed algorithm, in one iteration the same calculation is performed $n_{MCS} \times n_{CUR} \times M$ times. Note that the GA algorithm is only an initialization phase where ratios are fixed. Thus, we need $n_{MCS} \times 1 \times M$ times of the same calculation. As we will see in the next Section, the number of BRD iterations is relatively small, ensuring the practicality of the used BRD algorithm.

In Table 5, we summarize the complexity of different allocation methods to be presented in the next Section. This table includes the allocation using exhaustive search, BRD, GA allocations with fixed and variable channel use ratios. In this table, we present the complexity and the performance of these methods showing the importance of the BRD algorithm being a practical method with lower complexity and that approaches the benchmark of the complex exhaustive search approach.

Note that in all these methods, the calculation of outage events is included. So, in the case of SLA, the number of Monte-Carlo iterations used for calculating the outage events has a role in the convergence speed. However, it is seen in the next Section that the different allocation methods are robust to the number of samples taken. The only

comment to mention is that the use of MU encoding would lead to heavier computation as compared to the MU case, which ensures the motivation behind investigating the practical SU encoding case. Nevertheless, this issue is outside of the scope of this paper because it does not depend on the rate allocation and is to be visited in future works.

5 Results and discussion

In this Section, we present the performance results of several scenarios using Monte-Carlo simulations. We consider the (3,3,1)-MAMRN, with T_{\max} fixed to 4. In addition, we assume independent Gaussian distributed channel inputs (with zero mean and unit variance), with $I_{a,b} = \log_2(1 + |h_{a,b}|^2)$. Note that some other formulas could be also used for calculating $I_{a,b}$ where for example discrete entries, finite length of the code-words, non-outage achieving Joint Network Channel Coding/Joint Network Channel Decoding (JNCC/JNCD) architectures etc. would be taken into account. In addition, we can calibrate the mutual information by using weight factors as in [102]. As mentioned in [103], our main conclusions would still apply to these different functions of mutual information.

Moreover, we adopt an asymmetric link configuration setting, where each link has a different average SNR. The average SNR of each link is obtained from a unique value γ following the ordered steps:

- 1 All links are set to γ .
- 2 Links including source 2 are set to $\gamma-4$ dB.
- 3 Links including source 3 are set to $\gamma-7$ dB.
- 4 Links including both sources 2 and 3 are set to $\gamma - 5$ dB.

We carefully chose such kind of asymmetric configuration in order to make source 1 the source with the best links, followed by source 2, and source 3 is the source in the worst conditions (check [16]). We recall that the destination scheduling strategy is the one described in [98], i.e., in each retransmission round the selected node is the one that has i) the highest mutual information with the destination and ii) which can help (its decoding set includes at least one message that has not yet been decoded correctly by the destination). The set of rates and ratios used are $\{0, 0.75, 1.5, 2.25, 3, 3.75\}$ [bits per channel use], and $\{0.1, 0.55, 1, 1.45, 1.9\}$, respectively.

We define two QoS scenarios. QoS¹: $\Pr(O_{i,T_{\text{used}}}=1) \leq BLER_{\text{QoS},i} = 1$, and $R_i \geq R_{\min,i} = 0$ [bits per channel use], $\forall i \in \{1, \dots, M\}$. QoS²: where $R_{\min,i} = 0.5$ [bits per channel use] and $BLER_{\text{QoS},i} = 10^{-3} \forall i \in \{1, \dots, M\}$. Clearly, with QoS¹, no constraint is taken into consideration. Note that although we investigated many different QoS constraints, we chose these two QoS scenarios since we believe they cover two representative cases: no constraint and a severe constraint. As mentioned before, for FLA, we only use QoS¹. This is due to the fact that since the full CSI is known at the destination, it is possible to avoid any individual outage per frame by simply not transmitting or, equivalently, transmitting with zero rate. In SLA on the contrary, we investigate both cases, no constraint (i.e., QoS¹) and a severe constraint (i.e., QoS²).

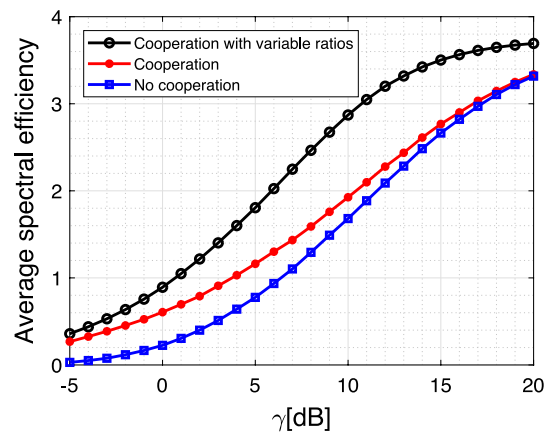
We divide the results into two main parts. In part 1, we investigate the effect of the new degree of freedom of variable number of channel uses at the transmission phase.

There, we check the gain of the proposed idea, and we investigate how this gain is changing with respect to the channel conditions and the system parameters (e.g., number of sources and number of relays). In part 2, we investigate the performance of the BRD algorithm allocating the rate and the channel uses for the sources. The performance is compared with an exhaustive search approach for both MU and SU encoding. We also test the practicality of the algorithm with respect to the channel conditions, number of samples needed, and the system parameters.

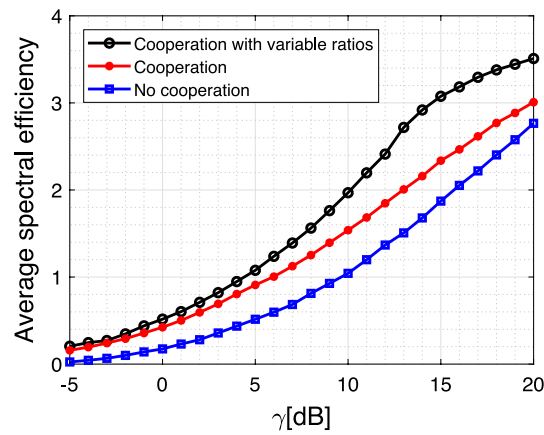
In the first part, we compare the ASE with respect to γ of 3 communication schemes, namely, no cooperation, cooperation, and cooperation with variable ratios. In the case of no cooperation, T_{\max} is fixed to zero, meaning that we only have a transmission phase, and no notion of cooperation or retransmission is included. For the case of cooperation, the ratios of all the sources are fixed to 1 (the average value of the possible ratio set). Then, at each retransmission time slot, the scheduling strategy is the one recalled above [98]. Finally, for the case of cooperation with variable ratios, the channel use ratios are optimized per source exploiting the proposed degree of freedom.

In Fig. 5, we see the performance of the three schemes: no cooperation ($T_{\max} = 0$), cooperation ($T_{\max} = 4$) with fixed ratios ($\alpha = 1$), and cooperation with variable ratios (α is optimized per source node) with: (a) FLA with QoS^1 , (b) SLA with QoS^1 , and (c) SLA with QoS^2 . In the FLA scenario (i.e., in Fig. 5a), the gain of cooperation with fixed ratios compared with no cooperation increases for low SNR values (low γ). This gain decreases for high SNR values. On the other hand, and upon introducing variable ratios at the transmission phase, the gain of cooperation increases and become significant over all the considered SNR range (-5dB to 20 dB). In Fig. 5b, a similar performance is seen with SLA with QoS^1 . Once again, optimizing the channel use at the transmission phase is leading to a significant gain compared with fixed channel use and with no cooperation at all. Finally, in Fig. 5c, the performance of the three schemes is presented for SLA with QoS^2 . Upon using this severe constraint, we see that with no cooperation, the system is always in outage. In other words, no possible allocation can be used to achieve the required constraint. On the other hand, upon using cooperation and cooperation with optimized channel use allocation, we see that starting from $\gamma = 4$ dB, the system is not in outage. Here again, optimizing α per source is leading to a better performance over all the considered SNR range larger than $\gamma = 4$ dB. To summarize, Fig. 5 gives the following findings: 1- using cooperation can help improve the performance, and is necessary with severe QoS constraints; 2- optimization of the channel use ratio can further improve the performance leading to a significant gain compared to fixed ratios scheme. Indeed, one obvious finding is that the ASE improves with increasing of the SNR, but the main goal of this figure is to ensure the significant improvement of cooperation. It is good to mention that with other QoS constraints (not presented here for brevity), a similar performance is seen. Simply, the performance of the different strategies slightly changes. For example, the γ level where the curves starts to be greater than zero is changed (for QoS^2 , $\gamma = 5$). With QoS smaller than QoS^2 , the γ level would be higher than 5, and with QoS higher than QoS^2 , the γ level would be smaller than 5.

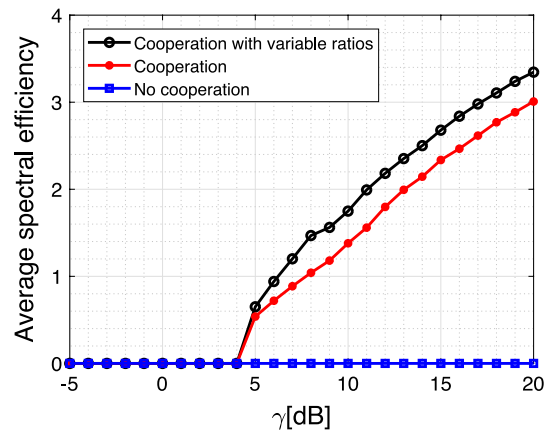
It is true that one obvious finding seen in our numerical results is that the spectral efficiency improves with increasing SNR (this is seen in Figs. 5, 8, 9). Nevertheless, this is not our intention to present. As mentioned in the text in the numerical results, the



(a) FLA with QoS^1 target



(b) SLA with QoS^1 target



(c) SLA with QoS^2 target

Fig. 5 ASE that corresponds to the proposed link adaptation algorithm for different scenarios

aim of Fig. 5 is to compare the performance of different schemes (using no cooperation, using cooperation, and using cooperation with variable ratios). Similarly in Fig. 8, our goal was to present the performance of the different LA algorithms. Finally, in Fig. 9,

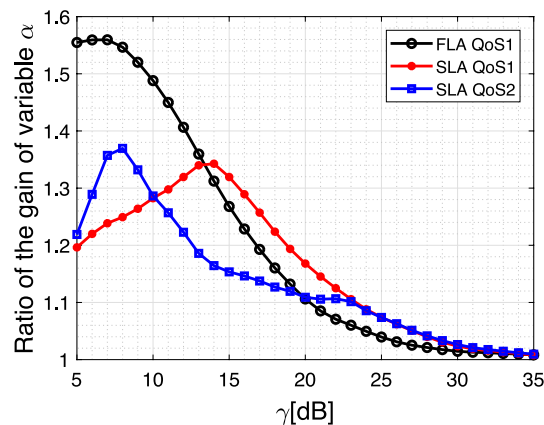


Fig. 6 The ratio of the ASE with variable α and fixed α with respect to γ

the aim was to show that a low number of MC simulation is enough to ensure the convergence of the BRD algorithm. On the other hand, we have several results that are not based on the increasing of the SNR (this is seen in Figs. 7, 10 for example). Thus, yes, one finding in our numerical result Section is that the spectral efficiency improves with increasing SNR, but our aim in the presented results is presented within the text of the manuscript. Following this comment of the reviewer, we added some comments in the numerical results Section to present and highlight the achievements of the article more clearly.

To our interest, we aim to investigate the operational conditions under which the gain of the proposed degree of freedom (variable ratio) is significant. Also, we aim to investigate this gain for different channel conditions (e.g., high SNR), and different system parameters. Accordingly, in the next two figures, we present the ratio of the (ASE with optimized α) and the (ASE with the fixed α). We present this ratio for the three cases: FLA, SLA with QoS¹, and SLA with QoS².

In Fig. 6, the ratio presenting the gain of variable α compared with fixed α is seen over the SNR range (5dB to 35dB). We aim here to investigate how the gain is changing for high SNR values. We see that for the three different LA considered, the gain is acting in a similar way. The gain starts to increase from low SNR values reaching its peak at an intermediate SNR value, and then it decreases for high SNR reaching the ratio 1 (meaning that we have no gain). To explain this asymptotic behavior, we recall that at high SNR, the destination is able to decode all the messages sent by all the sources no matter what rate or ratio is being used. Accordingly, the difference between the channel conditions of the different sources is insignificant (all sources are facing similar channel conditions of high SNR). Moreover, having a fixed possible rates and possible channel ratios sets, will lead to a limitation of the gain. For the rates, the destination will select the highest possible rate for all the sources. And finally, upon having a fixed rate for all the sources, the channel use allocation will be indifferent.

Such analysis can also be deduced directly by analyzing the spectral efficiency per frame equation [i.e., Eq. (2)]. Following that equation, and at high SNR, we can fix R_i to R_{\max} , and we can fix the outage and the T_{used} to zero (at high SNR there is no outage and

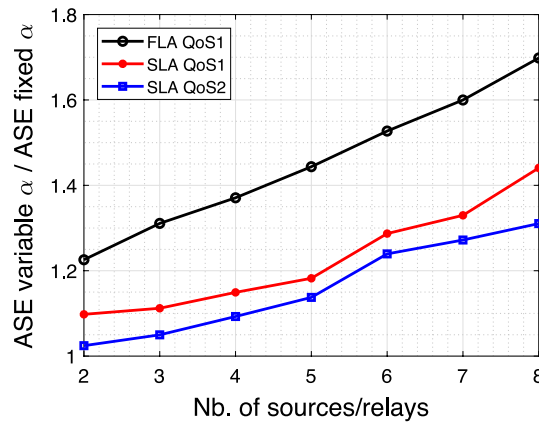


Fig. 7 The ratio of the ASE with variable α and fixed α with respect to network size

no need for retransmission phases). Then, it is directly seen that the ASE is limited to R_{\max} which justifies why we reach no gain at high SNR.

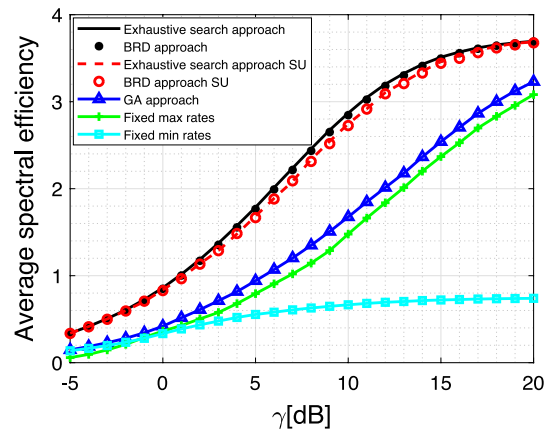
A final comment about the ratio at low SNR. As we see in the previous figure (i.e., Fig. 5) the ASE at low SNR is very small (and sometimes equal to zero), accordingly checking the ratio (ASE variable α /ASE fixed α) for such small values is not important. In other words, at low SNR, we might have a gain which is big, just because the ASE is very small. This might mislead to the conclusion that the proposed degree of freedom is important at low SNR. On the contrary, we say that after checking both the ASE and the ratio (ASE variable α /ASE fixed α), the proposed degree of freedom is most significant at intermediate SNR values.

Following Fig. 6, the gain is most significant in the range of 5dB to 15dB. Accordingly, in Fig. 7, we fix γ to 10dB and we investigate the effect of the number of sources and relays on the gain of the variable channel uses. The x-axis represents the value of M and L considered. In other words, for a given x , we consider a $(x,x,1)$ MAMRN. Note that we are still in an asymmetric link configuration, and for any value of M/L , the links of the sources are organized in a way making source i in better channel conditions from source j for $i < j$. Specifically, for a $(x,x,1)$ system, the average SNR of each link is obtained from a unique value $\gamma = 10$ following the ordered steps:

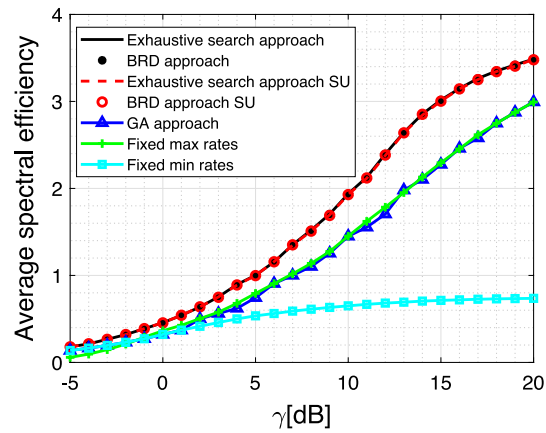
- 1 All links are set to γ .
- 2 The links including source $i \in \{1, \dots, x\}$ are set to $\gamma - 2(i - 1)$ dB.

For the three considered schemes (FLA, SLA with QoS¹, SLA with QoS²), we see that the gain of using variable ratios increases with the increase of the number of sources and relays. Also, we notice that the gain is approximately linear with respect to the size of the system. For FLA, the gain ratio reaches 1.7 with (8,8,1) system, whereas for SLA, the ratio is 1.45 and 1.3 with QoS¹ and QoS² respectively. This concludes the first part of simulations. So to summarize, our findings are

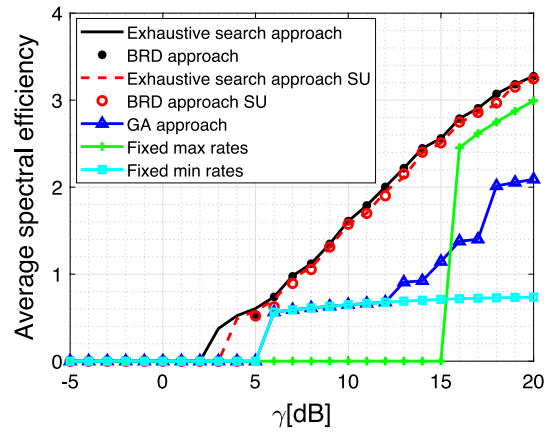
- Using cooperation (with fixed ratios or variable ratios) can improve the spectral efficiency and is a must for severe QoS constraints.



(a) FLA with QoS^1 target



(b) SLA with QoS^1 target



(c) SLA with QoS^2 target

Fig. 8 ASE that corresponds to the different algorithms with a variable α

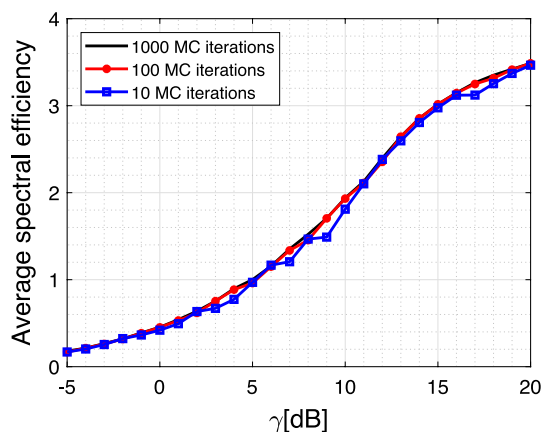


Fig. 9 ASE of BRD approach under SLA QoS¹ for different number of Monte-Carlo samples

- Using a variable number of channel uses at the transmission phase can help improve the spectral efficiency.
- The gain of using the new degree of freedom is mostly significant for intermediate SNR values. This gain is limited at high SNR following the highest possible rate value in the set of possible rates considered.
- The gain of variable channel uses increases with the increase in the system considered (i.e., with an increase of the number of sources and relays).

Keeping the same parameter settings used in the first part of simulations, and specifically the configurations used in Fig. 5, we now evaluate the performance of the BRD LA algorithm for α optimized per source with respect to other possible LA strategies including the LA utility metric optimization based on the exhaustive search approach. In particular, seven algorithms are presented:

- Exhaustive search approach: acting as the performance upper bound (exhaustive search over the possible vectors of pairs $\{\alpha, \text{rate}\}$). This algorithm is presented for the MU and the SU encoding.
- Best-Response Dynamic algorithm. Again, this algorithm is presented for the MU and the SU encoding.
- Genie Aided approach: being the starting point of the BRD algorithm in the MU case.
- Maximum Rate approach: a trivial approach using the average α and the maximum rate available (3.75 [bits per channel use]).
- Minimum Rate approach: a trivial approach using the average α and the minimum positive rate available (0.75 [bits per channel use]).

Here again, we present the results of FLA, SLA with QoS¹ target, and SLA with QoS² target. It is evident that in the three different scenarios, the proposed BRD algorithm converges to the optimal exhaustive search approach in both cases: the MU and the SU encoding. In addition, we notice that the GA approach leads to a loss of around 7 dB in the FLA case (Fig. 8a), at most 5 dB in the SLA with QoS¹target (Fig. 8b), and at most

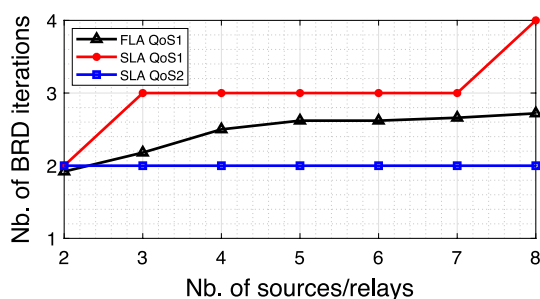


Fig. 10 The (average) number of BRD iterations with respect to sources/relays included in the system

5 dB in the SLA with QoS² target (Fig. 8c). Concerning the fixed allocation strategies, the minimum rate approach is always left behind. On the other hand, the fixed max rate approach gives a close performance to the GA approach when there is no QoS constraint (as in Fig. 8a, b) and an unacceptable performance with a severe QoS constraint (as in Fig. 8c) except for very high SNR.

This result confirms the performance of the practical low-complexity BRD algorithm. Even with a varying number of channel uses at the transmission phase, the BRD algorithm is approaching the complex exhaustive search approach. In addition, this result validates the observation in [22] that the SU encoding strategy while being much simpler behaves similarly to its MU counterpart, and thus presents a great interest in practice since the shelves capacity approaching IR codes can be used. Shorty, this result validates the performance of the BRD for both the MU and the SU case. In the next two figures, we investigate two other aspects of the BRD. In Fig. 8, we validate its performance, which gives an ASE close to the upper bound. Next, we investigate its practicality, in terms of the needed number of Monte-Carlo iterations and the number of BRD iterations.

In SLA, the BRD algorithm is performed based on the CDI of the channel conditions. According, a number of samples are needed to be simulated at the destination in order to calculate the *argmax* seen in step 8 of Algo. 2. In Fig. 9, we present the ASE for SLA with QoS¹ while using 10, 100, and 1000 Monte-Carlo samples. As we see in this figure, the ASE is slightly changing with respect to the number of MC samples used. Specifically, even 10 iterations were enough to reach acceptable performance. We conclude that the Monte-Carlo method is robust to the number of samples. Note that this results is also seen with different QoS constraints (e.g., QoS²), but we just show it with QoS¹.

Finally, in Fig. 10, we vary again the size of the system by varying the number of sources and relays used. The link configuration is similar to the one described in Fig. 7. Here, we investigate the number of BRD iterations used before reaching convergence. It is well known that the BRD algorithm will converge since the number of possible rates and ratios are finite. In the previous results (Fig. 8), we validate that the BRD convergence value is approaching the optimal value. In Fig. 9, we validate the practicality of the BRD algorithm being able to be performed using a low number of MC simulations. Finally, in Fig. 10, we validate the convergence speed by presenting the number of iterations the BRD algorithm is using for each (x,x,1)-MAMRN.

In Fig. 10, we see that for the three scenarios (FLA, SLA with QoS1, and SLA with QoS2) the number of BRD iterations is relatively small. Since in FLA the LA is performed

at each new CSI, we present the average number of BRD iterations used. On the contrary, since in SLA the LA is performed over a fixed CDI, we present the exact number of BRD iterations used. In both FLA, SLA QoS¹, and SLA with QoS², the number of iterations used is robust. For FLA, we see that the average number of iterations used is less than 3 iterations in all the considered systems up to (8,8,1)-MAMRN. Similarly in SLA, we see that with QoS¹, the highest number of iterations used was 4, and for SLA with QoS², the number of iterations used was always 2. It is seen that upon having a constraint, fewer options are available to the BRD algorithm, leading to a faster convergence than no constraint scenario.

This concludes the second part of simulations. So to summarize, our findings are

- The BRD algorithm is approaching the exhaustive search approach while tackling both rate and ratio allocation.
- The performance is similar for the MU and the SU encoding, which is interesting due to the practicality of the SU encoding case.
- In SLA, the Monte-Carlo method is robust to the number of samples needed, where only 10 iterations were sufficient in the presented scenario.
- The number of BRD iterations is slow in all the considered systems (up to (8,8,1)) which again validates the practicality of the considered algorithm.

6 Conclusion

In this paper, we investigate different LA algorithms for orthogonal MAMRN conditioned on the available channel information at the destination. Adapting the time slot duration of each source during the transmission phase is considered as a new degree of freedom. The LA algorithms find the rates and the time slot duration of each source in order to optimize the ASE of the system under per source QoS constraints. Both SLA and FLA are investigated, as well as MU encoding and the SU encoding sub-case. Monte Carlo Simulations show the significant impact of user cooperation on the spectral efficiency (up to 4 dB shift) as well as the importance of exploring the degree of freedom of the time slot duration associated with each source during the first transmission phase (up to 6dB shift). This gain is seen to be increasing with the size of the system (number of relaying nodes) and is limited to the maximum possible rate value. Furthermore, the numerical results validate the proposed BRD strategies (including a Genie Aided initial point determination), which tackle the complexity issue of the LA utility metric optimization. We see that the efficiency of the proposed algorithms holds in both cases: SLA and FLA, and in both encoding strategies: MU and SU encoding. We also see the practicality of the proposed solution being robust to the number of MC samples and facing a low number of BRD iterations. Future work may include tackling some novel relay selection strategies. Although the selection proposed in [98] is promising and useful in MU encoding strategy, it does not exploit the multi-path degree of freedom if SU encoding is used. As we validated that SU is performing in a close manner to MU, a novel selection strategies for SU encoding might be interesting. Another interesting work would be to investigate the rate allocation problem while using clustering within the source nodes. In

such a case, the rate allocation strategy would be simplified by reducing the allocation to the number of clusters of users.

Abbreviations

LA	Link adaptation
MAMRN	Multiple access multiple relay networks
BRD	Best-response dynamic
UAV	Unmanned aerial vehicle
TRN	Three-terminal relay network
MRN	Multiple relay network
RBN	Relay broadcast network
MARN	Multiple access relay network
DF	Decode-and-forward
SDF	Selective decode-and-forward
DDF	Dynamic decode-and-forward
CF	Compress-and-forward
CoF	Compute-and-forward
QMF	Quantize-map-and-forward
AF	Amplify-and-forward
NOAF	Non-orthogonal amplify-and-forward
RP	Relaying protocols
CC	Coded cooperation
CRC	Cyclic redundancy check
DMT	Diversity-multiplexing trade-off
TWRC	Two-way relay channel
NOMA	Non-orthogonal multiple access
NF	Neuro-fuzzy
MAB	Multi-armed bandit
TS	Thompson sampling
CMAB	Combinatorial MAB
CSMAB-F	Combinatorial sleeping MAB model with fairness constraints
FDM	Frequency division multiplexing
TDM	Time division multiplexing
QoS	Quality of service
BLER	Block error rate
ASE	Average spectral efficiency
SUCB1	Sequential upper confidence bound 1
MU	Multi-user
SU	Single-user
HARQ	Hybrid automatic repeat reQuest
JNCC	Joint network channel coding
IR	Incremental redundancy
CSI	Channel state information
CDI	Channel distribution information
SNR	Signal-to-noise ratio
SLA	Slow-link adaptation
FLA	Fast-link adaptation
GA	Genie-aided
MC	Monte-Carlo
MCS	Modulation and coding schemes
CUR	Channel use ratios
BER	Bit error rate
S-D	Source-to-destination
R-D	Relay-to-destination
S-S	Source-to-source
S-R	Source-to-relay
R-R	Relay-to-relay
ML	Maximum likelihood
JNCD	Joint network channel decoding

Acknowledgements

The authors would like to thank Miss Rasha Alkhansa for her help in several discussions as well as in proofreading the manuscript.

Author contributions

SC and RV were the first to work on this problem. They introduce the initial solutions including the Genie Aided idea and some different methods for the following sequential correction step. Specifically, SC did some part of the literature review, and RV proposed exploiting the degree of freedom of making the channel use variable in the transmission phase. Then, YH and SL then introduced the sequential BRD steps to solve the rate and channel use allocation. Specifically, SL

proposed several directions to improve the manuscript, especially in the numerical analysis study. Finally, the corresponding author was part of all the mentioned steps (set up of the problem, possible solutions, literature review). In addition, AAK was responsible for the writing of the manuscript as well as doing the numerical simulations. All authors read and approved the final manuscript.

Funding

Personal funding. There are no funding from the external organizations.

Availability of data and materials

Data sharing is not applicable to this article as no data sets were generated or analyzed during the current study.

Declarations

Competing interests

The authors declare that they have no competing interests.

Received: 13 May 2022 Accepted: 9 April 2023

Published online: 17 June 2023

References

1. G. Kramer, I. Marić, R.D. Yates, Cooperative communications. *Found. Trends Netw.* **1**(3), 271425 (2006). <https://doi.org/10.1561/1300000004>
2. R. Xue, L. Han, H. Chai, Complex field network coding for multi-source multi-relay single-destination UAV cooperative surveillance networks. *Sensors* **20**(6), 1542 (2020)
3. S. Nasrollahi, S.M. Mirrezaei, Toward UAV-based communication: improving throughput by optimum trajectory and power allocation. *EURASIP J. Wirel. Commun. Netw.* **2022**(1), 1–16 (2022)
4. EC Van Der Meulen, Three-terminal communication channels. *Adv. Appl. Probab.* **3**(1), 120–154 (1971)
5. T. Cover, A.E. Gamal, Capacity theorems for the relay channel. *IEEE Trans. Inf. Theory* **25**(5), 572–584 (1979)
6. A. El Gamal, T.M. Cover, Multiple user information theory. *Proc. IEEE* **68**(12), 1466–1483 (1980)
7. A. El Gamal, On information flow in relay networks, in *ntc*, vol. 2, (1981), pp. D4–1
8. M. R. Aref, Information flow in relay networks, Ph.D. (1981)
9. D.-W. Yue, H.H. Nguyen, Orthogonal df cooperative relay networks with multiple-snr thresholds and multiple hard-decision detections. *EURASIP J. Wirel. Commun. Netw.* **2010**, 1–11 (2010)
10. G. Kramer, M. Gastpar, P. Gupta, Cooperative strategies and capacity theorems for relay networks. *IEEE Trans. Inf. Theory* **51**(9), 3037–3063 (2005)
11. G. Kramer, A. J. van Wijnngaarden, On the white Gaussian multiple-access relay channel, in *2000 IEEE International Symposium on Information Theory* (Cat. No. 00CH37060) (IEEE, 2000), p. 40
12. L. Sankaranarayanan, G. Kramer, N. B. Mandayam, Capacity theorems for the multiple-access relay channel, in *Proceedings of 42nd Annual Allerton Conference on Communication, Control, and Computing* (2004), pp. 1782–1791
13. L. Sankaranarayanan, G. Kramer, N. B. Mandayam, Hierarchical sensor networks: capacity bounds and cooperative strategies using the multiple-access relay channel model, in *2004 First Annual IEEE Communications Society Conference on Sensor and Ad Hoc Communications and Networks, 2004. IEEE SECON 2004* (IEEE, 2004), pp. 191–199
14. S. Cerovic, Cooperative wireless communications in the presence of limited feedback, Ph.D. dissertation, Université Paris-Saclay (2019)
15. A. Mohamad, Cooperative relaying protocols and distributed coding schemes for wireless multiterminal networks, Theses, Université Paris-Saclay, May (2016). [Online]. <https://tel.archives-ouvertes.fr/tel-01349387>
16. S. Cerovic, Cooperative wireless communications in the presence of limited feedback, Theses, Université Paris-Saclay, Sep. (2019). [Online]. <https://tel.archives-ouvertes.fr/tel-02330710>
17. A. Mohamad, R. Visoz, A.O. Berthet, Outage achievable rate analysis for the non orthogonal multiple access multiple relay channel, in *IEEE Wireless Communications and Networking Conference Workshops (WCNCW)* (IEEE, 2013), pp. 160–165
18. A. Mohamad, R. Visoz, A. O. Berthet, Outage analysis of various cooperative strategies for the multiple access multiple relay channel, in *IEEE 24th Annual International Symposium on Personal, Indoor, and Mobile Radio Communications (PIMRC)* (IEEE, 2013), pp. 1321–1326
19. A. Mohamad, R. Visoz, A.O. Berthet, Outage analysis of dynamic selective decode-and-forward in slow fading wireless relay networks, in *8th International Congress on Ultra Modern Telecommunications and Control Systems and Workshops (ICUMT)* (IEEE, 2016), pp. 420–426
20. A. Mohamad, R. Visoz, A.O. Berthet, Dynamic selective decode and forward in wireless relay networks, in *7th International Congress on Ultra Modern Telecommunications and Control Systems and Workshops (ICUMT)* (IEEE, 2015), pp. 189–195
21. S. Cerovic, R. Visoz, L. Madier, A. O. Berthet, Centralized scheduling strategies for cooperative harq retransmissions in multi-source multi-relay wireless networks, in *2018 IEEE International Conference on Communications (ICC)* (IEEE, 2018), pp. 1–6
22. S. Cerović, R. Visoz, L. Madier, Efficient cooperative harq for multi-source multi-relay wireless networks, in *2018 14th International Conference on Wireless and Mobile Computing, Networking and Communications (WiMob)* (IEEE, 2018), pp. 61–68
23. A. Sendonaris, E. Erkip, B. Aazhang, User cooperation diversity. Part I. system description. *IEEE Trans. Commun.* **51**(11), 1927–1938 (2003)

24. A. Sendonaris, E. Erkip, B. Aazhang, User cooperation diversity. Part II. Implementation aspects and performance analysis. *IEEE Trans. Commun.* **51**(11), 1939–1948 (2003)
25. J.N. Laneman, D.N. Tse, G.W. Wornell, Cooperative diversity in wireless networks: efficient protocols and outage behavior. *IEEE Trans. Inf. Theory* **50**(12), 3062–3080 (2004)
26. M.R. Javan, N. Mokari, F. Alavi, A. Rahmati, Resource allocation in decode-and-forward cooperative communication networks with limited rate feedback channel. *IEEE Trans. Veh. Technol.* **66**(1), 256–267 (2016)
27. K. Azarian, H. El Gamal, P. Schniter, On the achievable diversity-multiplexing tradeoff in half-duplex cooperative channels. *IEEE Trans. Inf. Theory* **51**(12), 4152–4172 (2005)
28. G. Kramer, M. Gastpar, P. Gupta, Cooperative strategies and capacity theorems for relay networks. *IEEE Trans. Inf. Theory* **51**(9), 3037–3063 (2005)
29. S.H. Lim, Y.H. Kim, A.E. Gamal, S.Y. Chung, Noisy network coding. *IEEE Trans. Inf. Theory* **57**(5), 3132–3152 (2011)
30. B. Nazer, M. Gastpar, Compute-and-forward: harnessing interference through structured codes. *IEEE Trans. Inf. Theory* **57**(10), 6463–6486 (2011)
31. L. Wei, W. Chen, Compute-and-forward network coding design over multi-source multi-relay channels. *IEEE Trans. Wireless Commun.* **11**(9), 3348–3357 (2012)
32. A.S. Avestimehr, S.N. Diggavi, D.N.C. Tse, Wireless network information flow: a deterministic approach. *IEEE Trans. Inf. Theory* **57**(4), 1872–1905 (2011)
33. J. N. Laneman, Cooperative diversity in wireless networks: algorithms and architectures, Ph.D. dissertation, Massachusetts Institute of Technology, Cambridge, MA (2002)
34. P. Hao, X. Wang, A. Behnad, Amplify-and-forward relay identification using joint Tx/Rx I/Q imbalance-based device fingerprinting. *EURASIP J. Wirel. Commun. Netw.* **2019**(1), 1–16 (2019)
35. M. Janani, A. Hedayat, T.E. Hunter, A. Nosratinia, Coded cooperation in wireless communications: space-time transmission and iterative decoding. *IEEE Trans. Signal Process.* **52**(2), 362–371 (2004)
36. Q. Y. Liao, C. Y. Leow, Amplify-and-forward relay selection in cooperative non-orthogonal multiple access, in *2017 IEEE 13th Malaysia International Conference on Communications (MICC)* (IEEE, 2017), pp. 79–83
37. S. Xu, D. Xu, Fountain codes-based two-way multiply-and-forward relaying in Rayleigh fading channels, in *2020 IEEE International Conference on Artificial Intelligence and Information Systems (ICAIIIS)* (IEEE, 2020), pp. 781–784
38. J.N. Laneman, G.W. Wornell, Distributed space-time-coded protocols for exploiting cooperative diversity in wireless networks. *IEEE Trans. Inf. Theory* **49**(10), 2415–2425 (2003)
39. J.N. Laneman, D.N.C. Tse, G.W. Wornell, Cooperative diversity in wireless networks: efficient protocols and outage behavior. *IEEE Trans. Inf. Theory* **50**(12), 3062–3080 (2004)
40. T.Q. Duong, H.-J. Zepernick, On the performance gain of hybrid decode-amplify-forward cooperative communications. *EURASIP J. Wirel. Commun. Netw.* **2009**, 1–10 (2009)
41. R. Ahlswede, N. Cai, S.Y.R. Li, R.W. Yeung, Network information flow. *IEEE Trans. Inf. Theory* **46**(4), 1204–1216 (2000)
42. C. Hausl, P. Dupraz, Joint network-channel coding for the multiple access relay channel, in *Proceedings of IEEE SECON'06*, Reston, VA, USA, September (2006)
43. C. Hausl, J. Hagenauer, Iterative network and channel decoding for the two-way relay channel, in *Proceedings of IEEE ICC'06*, Istanbul, Turkey, June (2006)
44. L. Xiao, T.E. Fuja, J. Kliewer, D.J. Costello, A network coding approach to cooperative diversity. *IEEE Trans. Inf. Theory* **53**(10), 3714–3722 (2007)
45. O. Abujwa, M. Roslee, Z.B. Yusoff, L.L. Chuan, P.W. Leong, Resource allocation for throughput versus fairness trade-offs under user data rate fairness in NOMA systems in 5g networks. *Appl. Sci.* **12**(7), 3226 (2022)
46. F.K. Ojo, D.O. Akande, M.F.M. Salleh, Optimal power allocation in cooperative networks with energy-saving protocols. *IEEE Trans. Veh. Technol.* **69**(5), 5079–5088 (2020)
47. M. Pounambal, Survey on channel allocation techniques for wireless mesh network to reduce contention with energy requirement. *Indian J. Sci. Technol.* **9**(32), 1–12 (2016)
48. R. Yilmazel, N. Inanc, A novel approach for channel allocation in OFDM based cognitive radio technology. *Wirel. Pers. Commun.* **120**(1), 307–321 (2021)
49. X. Deng, J. Luo, L. He, Q. Liu, X. Li, L. Cai, Cooperative channel allocation and scheduling in multi-interface wireless mesh networks. *Peer-to-Peer Network. Appl.* **12**(1), 1–12 (2019)
50. Y. Liu, E. Erkip, Capacity and rate regions of a class of broadcast interference channels. *IEEE Trans. Inf. Theory* **62**(10), 5556–5572 (2016)
51. H. Qiu, S. Gao, Y. Chen, G. Tu, Energy-efficient rate allocation for NOMA-MEC offloading under outage constraints. *IEEE Commun. Lett.* **11**, 2710–2714 (2022)
52. H. Jung, A. R. Pedram, T. C. Cuvelier, T. Tanaka, Optimized data rate allocation for dynamic sensor fusion over resource constrained communication networks. *Int. J. Robust Nonlinear Control* **33.1**, 237–263 (2022)
53. S. Yin, Z. Qu, Resource allocation in cooperative networks with wireless information and power transfer. *IEEE Trans. Veh. Technol.* **67**(1), 718–733 (2017)
54. M.S. Kaiser, M.H. Chaudary, R.A. Shah, K.M. Ahmed, Neuro-fuzzy based relay selection and resource allocation for cooperative networks, in *ECTI-CON2010: The ECTI International Conference on Electrical Engineering/Electronics. Computer, Telecommunications and Information Technology* (IEEE, 2010), pp. 244–248
55. H. Zeng, X. Zhu, Y. Jiang, Z. Wei, S. Sun, X. Xiong, Toward UL-DL rate balancing: joint resource allocation and hybrid-mode multiple access for UAV-BS-assisted communication systems. *IEEE Trans. Commun.* **70**(4), 2757–2771 (2022)
56. S. Dayarathna, R. Senanayake, J. Evans, Maximizing sum-rate via relay selection and power control in dual-hop networks, in *IEEE Wireless Communications and Networking Conference (WCNC)* (IEEE, 2022), pp. 2340–2345
57. M. Naeem, A. Anpalagan, M. Jaseemuddin, D.C. Lee, Resource allocation techniques in cooperative cognitive radio networks. *IEEE Commun. Surv. Tutor.* **16**(2), 729–744 (2013)
58. A. Lozano, A.M. Tulino, S. Verdú, Optimum power allocation for parallel gaussian channels with arbitrary input distributions. *IEEE Trans. Inf. Theory* **52**(7), 3033–3051 (2006)
59. N. Papandreou, T. Antonakopoulos, Bit and power allocation in constrained multicarrier systems: the single-user case. *EURASIP J. Adv. Signal Process.* **2008**, 1–14 (2007)

60. S. Iqbal, A.H. Abdullah, K. Hussain, F. Ahsan, Channel allocation in multi-radio multi-channel wireless mesh networks: a categorized survey. *KSII Trans. Internet Inf. Syst. (TIIS)* **9**(5), 1642–1661 (2015)
61. V. Kumar, S. K. Dhurandher, B. Tushir, M. S. Obaidat, Channel allocation in cognitive radio networks using evolutionary technique, in *International Conference on Wireless Networks and Mobile Systems*, vol. 2 (SCITEPRESS, 2016), pp. 106–112
62. G. Zhao, C. Yang, G. Y. Li, D. Li, A. Soong, Channel allocation for cooperative relays in cognitive radio networks, in *2010 IEEE International Conference on Acoustics, Speech and Signal Processing (IEEE)*, 2010, pp. 3258–3261
63. S. Toumpis, A.J. Goldsmith, Capacity regions for wireless ad hoc networks. *IEEE Trans. Wirel. Commun.* **2**(4), 736–748 (2003)
64. M. Kodialam, T. Nandagopal, Characterizing the capacity region in multi-radio multi-channel wireless mesh networks, in *Proceedings of the 11th annual international conference on Mobile Computing and Networking*, pp. 73–87 (2005)
65. N. Akbar, N. Yang, P. Sadeghi, R.A. Kennedy, Multi-cell multiuser massive mimo networks: User capacity analysis and pilot design. *IEEE Trans. Commun.* **64**(12), 5064–5077 (2016)
66. S. Sridharan, S. Vishwanath, On the capacity of a class of mimo cognitive radios. *IEEE J. Sel. Top. Signal Process.* **2**(1), 103–117 (2008)
67. S. Bubeck, N. Cesa-Bianchi, Regret analysis of stochastic and nonstochastic multi-armed bandit problems, arXiv preprint [arXiv:1204.5721](https://arxiv.org/abs/1204.5721) (2012)
68. L. Weng, The multi-armed bandit problem and its solutions, [lilianweng.github.io/lil-log](https://github.com/lilianweng/lil-log), (2018)
69. W.R. Thompson, On the likelihood that one unknown probability exceeds another in view of the evidence of two samples. *Biometrika* **25**(3/4), 285–294 (1933)
70. D. Russo, B. Van Roy, A. Kazerouni, I. Osband, Z. Wen, A tutorial on thompson sampling, arXiv preprint [arXiv:1707.02038](https://arxiv.org/abs/1707.02038) (2017)
71. R. Combes, S. Magureanu, A. Proutiere, Minimal exploration in structured stochastic bandits, arXiv preprint [arXiv:1711.00400](https://arxiv.org/abs/1711.00400) (2017)
72. W.B. Ameur, P. Mary, J.-F. H elard, M. Dumay, J. Schwoerer, Autonomous power decision for the grant free access MUSA scheme in the MMTC scenario. *Sensors* **21**(1), 116 (2021)
73. I. Nasim, A.S. Ibrahim, S. Kim, Learning-based beamforming for multi-user vehicular communications: a combinatorial multi-armed bandit approach. *IEEE Access* **8**, 219891–219902 (2020)
74. V. Kuchibhotla, P. Harshitha, D. Elugoti, Combinatorial sleeping bandits with fairness constraints and long-term non-availability of arms, in *2020 4th International Conference on Electronics, Communication and Aerospace Technology (ICECA)* (IEEE, 2020), pp. 1575–1581
75. T.L. Lai, H. Robbins, Asymptotically efficient adaptive allocation rules. *Adv. Appl. Math.* **6**(1), 4–22 (1985)
76. S. Bubeck, Bandits games and clustering foundations, Ph.D. dissertation, INRIA Nord Europe (2010)
77. A. Garivier and O. Capp e, The kl-ucb algorithm for bounded stochastic bandits and beyond, in *Proceedings of the 24th Annual Conference on Learning Theory. JMLR Workshop and Conference Proceedings*, pp. 359–376 (2011)
78. O. Chapelle, L. Li, An empirical evaluation of Thompson sampling. *Adv. Neural. Inf. Process. Syst.* **24**, 2249–2257 (2011)
79. W. Chen, Y. Wang, Y. Yuan, Combinatorial multi-armed bandit: general framework and applications, in *International Conference on Machine Learning (PMLR)*, 2013, pp. 151–159
80. S. Zhang, B. Di, L. Song, Y. Li, Sub-channel and power allocation for non-orthogonal multiple access relay networks with amplify-and-forward protocol. *IEEE Trans. Wirel. Commun.* **16**(4), 2249–2261 (2017)
81. A. Zappone, Z. Chong, E.A. Jorswieck, S. Buzzi, Energy-aware competitive power control in relay-assisted interference wireless networks. *IEEE Trans. Wirel. Commun.* **12**(4), 1860–1871 (2013)
82. E.V. Belmega, B. Djeumou, S. Lasaulce, Power allocation games in interference relay channels: existence analysis of nash equilibria. *EURASIP J. Wirel. Commun. Netw.* **2010**, 1–20 (2010)
83. F. Shams, G. Bacci, M. Luise, Energy-efficient power control for multiple-relay cooperative networks using q -learning. *IEEE Trans. Wirel. Commun.* **14**(3), 1567–1580 (2014)
84. E.E. Tsiropoulou, P. Vamvakas, S. Papavassiliou, Joint utility-based uplink power and rate allocation in wireless networks: a non-cooperative game theoretic framework. *Phys. Commun.* **9**, 299–307 (2013)
85. U. Sharma, P. Mittal, C. Nagpal, Implementing game theory in cognitive radio network for channel allocation: an overview. *Int. J. Energy Inf. Commun.* **6**(2), 17–22 (2015)
86. S. Driouech, E. Sabir, M. Ghogho, E.-M. Amhoud, D2d mobile relaying meets nomapart I: a biform game analysis. *Sensors* **21**(3), 702 (2021)
87. S. Driouech, E. Sabir, M. Ghogho, E.-M. Amhoud, D2d mobile relaying meets nomapart II: a reinforcement learning perspective. *Sensors* **21**(5), 1755 (2021)
88. A. Al Khansa, R. Visoz, Y. Hayel, S. Lasaulce, R. Alkhansa, Centralized scheduling for frequency domain orthogonal multiple access multiple relay network, in *2022 27th Asia Pacific Conference on Communications (APCC)*, pp. 260–265 (2022)
89. V. Douros, S. Toumpis, G. C. Polyzos, Power control under best response dynamics for interference mitigation in a two-tier femtocell network, in *Proceedings of WIOpt* (2012)
90. Z. Han, D. Niyato, W. Saad, T. Ba sar, A. H jorungnes, *Game Theory in Wireless and Communication Networks: Theory, Models, and Applications* (Cambridge University Press, Cambridge, 2012)
91. I. Bistriz, A. Leshem, Convergence of approximate best-response dynamics in interference games, in *Proceedings of IEEE CDC* (2016)
92. S. Lasaulce, H. Tembine, *Game Theory and Learning for Wireless Networks: Fundamentals and Applications* (Academic Press, London, 2011)
93. S.-J. Kim, G.B. Giannakis, Optimal resource allocation for mimo ad hoc cognitive radio networks. *IEEE Trans. Inf. Theory* **57**(5), 3117–3131 (2011)
94. A. A. Khansa, R. Visoz, Y. Hayel, S. Lasaulce, Resource allocation for multi-source multi-relay wireless networks: A multi-armed bandit approach, in *International Symposium on Ubiquitous Networking* (Springer, 2021), pp. 62–75

95. A. Al Khansa, S. Cerovic, R. Visoz, Y. Hayel, S. Lasaulce, Slow-link adaptation algorithm for multi-source multi-relay wireless networks using best-response dynamics, in *International Conference on Network Games, Control and Optimization* (Springer, 2021), pp. 38–47
96. A. Al Khansa, R. Visoz, Y. Hayel, S. Lasaulce, R. Alkhansa, Fast link adaptation with partial channel state information for orthogonal multiple access multiple relay channel (OMAMRC), in *2021 IEEE 3rd International Multidisciplinary Conference on Engineering Technology (IMCET)* (IEEE, 2021), pp. 11–16
97. B. Zhang, C. Zhang, J. Mu, W. Wang, J. Xie, An adaptive relay node selection algorithm based on opportunity. *EURASIP J. Wirel. Commun. Netw.* **2017**(1), 1–8 (2017)
98. S. Cerovic, R. Visoz, L. Madier, A. O. Berthet, Centralized scheduling strategies for cooperative harq retransmissions in multi-source multi-relay wireless networks, in *Proceedings of IEEE ICC'18, Kansas City, MO, USA, May (2018)*
99. 3GPP, Revised WID on NR sidelink relay enhancements, in *3rd Generation Partnership Project (3GPP), Work Item Description 941002, 06 (2022)*
100. L.H. Ozarow, S. Shamai, A.D. Wyner, Information theoretic considerations for cellular mobile radio. *IEEE Trans. Veh. Technol.* **43**(2), 359–378 (1994)
101. T.M. Cover, *Elements of Information Theory* (Wiley, New York, 1999)
102. K. Brueninghaus, D. Astely, T. Salzer, S. Visuri, A. Alexiou, S. Karger, G.-A. Seraji, Link performance models for system level simulations of broadband radio access systems, in *IEEE 16th International Symposium on Personal, Indoor and Mobile Radio Communications*, vol. 4 (IEEE, 2005), pp. 2306–2311
103. Y. Polyanskiy, H.V. Poor, S. Verdú, Channel coding rate in the finite blocklength regime. *IEEE Trans. Inf. Theory* **56**(5), 2307–2359 (2010)

Publisher's Note

Springer Nature remains neutral with regard to jurisdictional claims in published maps and institutional affiliations.

Submit your manuscript to a SpringerOpen[®] journal and benefit from:

- Convenient online submission
- Rigorous peer review
- Open access: articles freely available online
- High visibility within the field
- Retaining the copyright to your article

Submit your next manuscript at ► [springeropen.com](https://www.springeropen.com)
